



HUMAN HEALTH

ENVIRONMENTAL HEALTH

SPOTLIGHT  
ON APPLICATIONS.  
FOR A BETTER  
TOMORROW.

VOLUME 8



**PerkinElmer**  
*For the Better*

## INTRODUCTION

### PerkinElmer Spotlight on Applications e-Zine – Volume 8

PerkinElmer knows that the right training, methods and application support are as integral to getting answers as the instrumentation. That's why PerkinElmer has developed a novel approach to meet the challenges that today's labs face, delivering you complete solutions for your application challenges.

We are pleased to share with you our *Spotlight on Applications* e-zine, which delivers a variety of topics that address the pressing issues and analytical challenges you may face in your application areas today.

Our *Spotlight on Applications* e-zine consists of a broad range of applications you'll be able to access at your convenience. Each application in the table of contents includes an embedded link which that take you directly to the appropriate page within the e-zine.

We invite you to explore, enjoy and learn!

► Be sure to receive future issues by subscribing here.

# CONTENTS

## Consumer Products

- Plasticizer Characterization by TG-IR
- Crystallization Temperature vs. Cooling Rate: the Link with “Real-Life” Polymer Processes



## Energy/Petrochemical

- The Determination of C<sub>2</sub> to C<sub>5</sub> Hydrocarbons in Finished Gasolines using the PerkinElmer Clarus 680 GC with Swafer Technology
- Analysis of UV-Curable Resins by FT-IR
- Cavity-enhanced Absorption Spectroscopy for Trace Gas Detection with Frontier
- Wax Appearance Temperature Detection by DSC



## Food & Beverage

- Investigating Phase Transitions with Variable Temperature ATR
- Analysis of the Mycotoxin Patulin in Apple Juice Using the Flexar FX-15 UHPLC-UV



## Forensics & Toxicology

- Determination of Aluminum in Serum in Customer-Validated Applications using THGA and Longitudinal Zeeman Atomic Absorption
- Using THGA and Zeeman Background Correction for Blood-Lead Determination in Customer-Validated Applications



## Pharmaceuticals & Nutraceuticals

- Rapid Authentication of Larch Fiber Dietary Supplement Ingredient by FT-IR Using Diamond Single Bounce uATR Sampling Device
- Pharmaceutical Compounds are Analyzed in Half the Time by Simultaneous TGA-DSC
- Solid Materials Checking Using the Near-IR Reflectance Accessory (NIRA)
- Rapid Authentication of Botanicals for Dietary Supplement cGMP's Compliance by Automated FT-NIR Using Chemometric Modeling



Thermogravimetric-  
Infrared Analysis

## Authors

Maria Grazia Garavaglia

Peng Ye

PerkinElmer, Inc.  
Shelton, CT 06484 USA

## Plasticizer Characterization by TG-IR

### Introduction

Plasticizers are additives that are added to polymeric material to increase flexibility. For example, phthalates are usually added to hard PVC plastics to make it soft. Many properties of the polymer will be changed by the addition of a plasticizer, such as the glass transition temperature (T<sub>g</sub>) which will be reduced dramatically; the hardness which will be reduced; the strength which will decrease and the processability which will be improved. Since

plasticizer is often made up of small molecules, it will migrate to the surface and evaporate from the polymer matrix over time or upon heating. One common example is the smell of a new car which is caused by the plasticizer evaporating from the car's interior polymer parts. Because the plasticizer may be toxic and be harmful to human health, restrictions often apply to some types of phthalates such as in children's toys in the United States and European Union. It may be important to know the plasticizer added to the polymer product and its content.

Thermogravimetric analysis (TGA) is a common technique that is used to study the weight loss during heating. It can tell you the percentage of weight loss quantitatively and accurately. But TGA alone will not tell you anything about the chemical components of the evolved off gas. The hyphenation between TGA and FT-IR is able to identify the off gas from TGA and give a more complete picture of material characterization.

In this note, the sample is a complex mixture of solvent, plasticizer and polymers from a paint and varnish producer who require data concerning the plasticizer and its percentage.

## Instrument

A PerkinElmer® Pyris™ 1 TGA and Spectrum™ 100 system connected by the state-of-the-art TL 8000 transfer line was used for this analysis (Figure 1).



Figure 1. The TL 8000 transfer line couples a Spectrum 100 FT-IR to a Pyris 1 TGA.

The advantages of this system include:

- Insulated heated transfer line with replaceable SilcoSteel® liner.
- Heated zero-gravity-effect 'ZGCell' gas cell for the Spectrum instrument incorporating automatic accessory identification, low volume, and efficient sample area purging.
- Control unit incorporating a mass flow controller, particle filters, flow smoothing system, independent transfer line and gas cell temperature controllers, and vacuum pump with exhaust line.
- Automatic triggering of IR data collection from the Pyris software.
- Spectrum Timebase software for time resolved experiments.

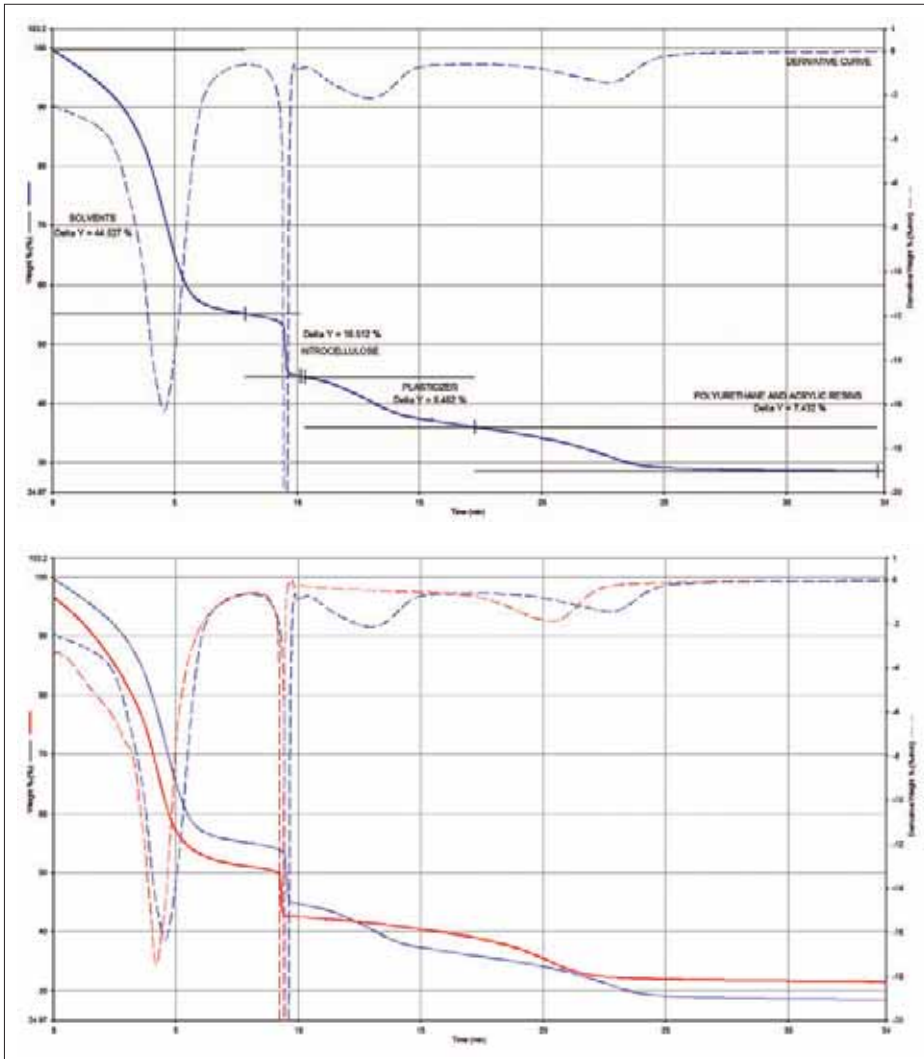


Figure 2. TGA and its derivative curve. Red curve: sample without plasticizer; Blue curve: sample with about 8% plasticizer.

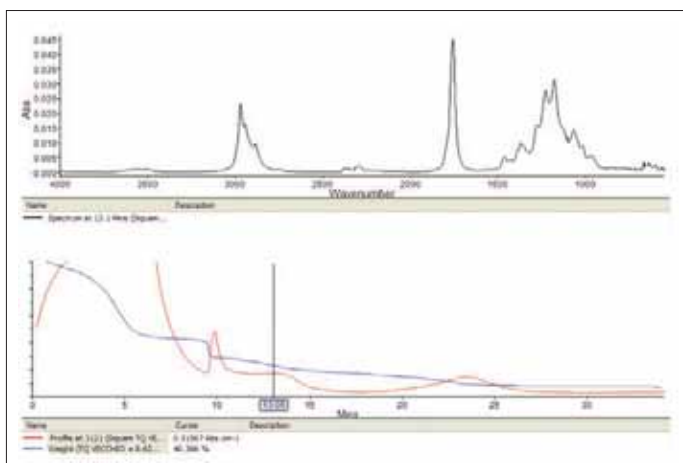


Figure 3. The IR spectrum at 13 minutes.

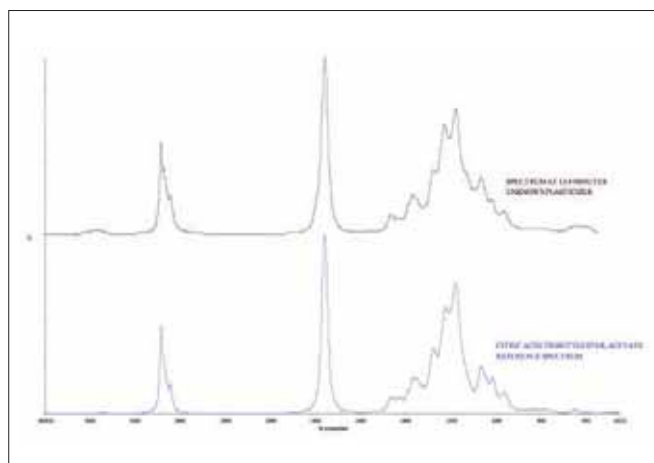


Figure 4. Unknown plasticizer spectrum vs. reference spectrum.

## Result

Two samples were analyzed by TG-IR. The red TGA curve is the sample without plasticizer; the blue TGA curve is the same sample with the addition of approximately 8% of plasticizer in Figure 2. The derivative of weight loss is also shown in order to help identify the weight loss event.

For the red curve, the first loss of weight is due to the solvents; the second loss is attributed to nitrocellulose polymer and the third loss is due to polyurethane + polyacrylate polymers. For the blue curve, the first loss is from solvents; the second loss is again from nitrocellulose polymer; the third loss is supposed to be from the added plasticizer and the fourth loss is from polyurethane + polyacrylate polymers. All components were identified from gaseous fragments in TG-IR. So by comparing the red curve with the blue curve, it can be seen that the only difference is the weight loss due to plasticizer from the blue curve. The content of plasticizer is determined to be 8.48%.

In order to identify the plasticizer, the IR spectrum is used in Figure 3. The IR spectrum at 13 minutes is used because from TGA curve it can be seen that the evolved gas at this point is from the plasticizer. By looking at this IR spectrum and comparing it to reference spectrum (Figure 4), it can be shown that the plasticizer used here is citric acid, tributylester, acetate.

## Conclusion

The TG-IR hyphenation technique has been widely used for the polymer industry, in this case the identification of plasticizer in paint. It combines the strength of TGA and FT-IR analysis and offers a more comprehensive material characterization. The PerkinElmer TG-IR system with the TL 8000 transfer line has proven to be the ideal solution for this analysis. It is easy to use and its design features guarantee the highest quality and most reliable results.

## Differential Scanning Calorimetry

## Authors

Geert Vanden Poel

DSM Resolve  
The Netherlands

Vincent B.F. Mathot

SciTe B.V.  
The Netherlands

Peng Ye

PerkinElmer, Inc.  
Shelton, CT 06484 USA

## Crystallization Temperature vs. Cooling Rate: the Link with “Real-Life” Polymer Processes

### Introduction

A relatively new technology for calorimetry has recently been discussed for practical use and since then marketed by PerkinElmer under the name HyperDSC<sup>®</sup>. The detailed characteristics and use of this new mode of measurement, which represents a major step forward in Fast Scanning Calorimetry (FSC) as compared to Standard DSC, have been published.<sup>1-4</sup> Controlled and constant scan rates of hundreds of degrees per minute and combinations thereof, both in the cooling and heating mode, are possible thanks to the small furnace size compared with the bulky furnace of the conventional heat flux DSC (Figure 1). Thanks to the power compensation design which supports accurate heat flow rate measurement, heats of transition, heat capacities, temperature-dependent crystallinities etc. can be established at the extreme rates applied. The short measuring times also provide the high throughput needed in e.g. combinatorial chemistry.

### PerkinElmer Power Compensation vs. Heat Flux



Figure 1. Furnace of HyperDSC versus heat flux DSC furnace.



Application fields benefiting from HyperDSC concern study of the kinetics and metastability of macromolecular and pharmaceutical systems, particularly the analysis of rate-dependent phenomena under real temperature-time conditions. Thus, HyperDSC is very much suited to investigate these systems with respect to their kinetics of processes such as crystallization, cold crystallization, recrystallization, annealing, and solid-state transformations.

Milligram and submilligram amounts of material can be investigated at controlled cooling and heating rates as high as hundreds of degrees per minute, which facilitates the analysis of films, expensive and extraordinary products, inhomogeneities in materials etc.

High cooling rates need to be applied to simulate processing conditions such as in film blow molding, injection molding and extrusion. It appears that for some processing techniques the cooling rate can be mimicked by HyperDSC. Measurements concerning metastability and kinetics are also necessary to (re)connect heating behavior with cooling history.

## Experimental

The PET/PBT samples reported have been supplied by DSM. DSC measurements were performed using a Diamond DSC (PerkinElmer) with an Intracooler II cooling accessory. Cooling rates of 10 to 250 °C/min have been used to study their effect on the crystallization behavior of the polymers involved. To keep the thermal lag minimal, the sample sizes were reduced with increasing cooling rates.

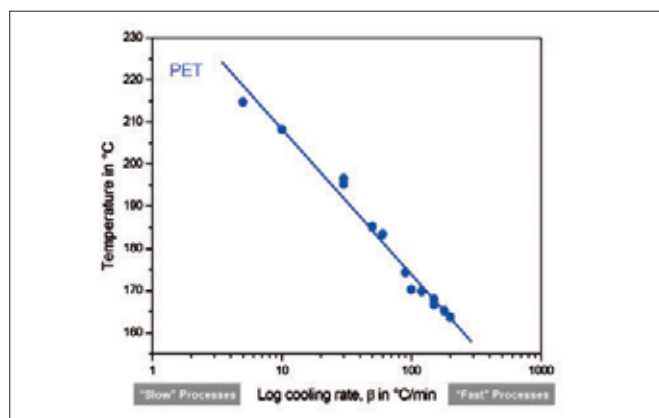


Figure 2. PET crystallization peak temperature as a function of log cooling rate.

## Results and Discussion

In industrial applications the crystallization temperature of a polymer is considered to be the temperature at which the polymer becomes solidified during processing. This temperature

is the limiting value for proper injection molding conditions for “real-life” applications. A polymer or compound which crystallizes “too fast” will solidify too soon resulting in a not-completely filled mold. If the polymer or compound crystallizes “too slow”, the release from the mold will be problematic.

Presenting a characteristic crystallization temperature as a function of the (log) cooling rate provides useful insight into the crystallization behavior of the material studied. Figure 2 shows the crystallization peak temperature of PET vs. log cooling rate. With increasing cooling rates, this temperature decreases significantly.

In case of polyethylene terephthalate (PET) and polybutylene terephthalate (PBT), Standard DSC experiments at relatively slow cooling rates suggest that PET will crystallize prior to PBT. However, when measured during fast cooling by means of HyperDSC it is seen that one should expect that PBT crystallizes first, followed by PET (Figure 3). Thus, it is obvious that in many cases fast scanning represents realistic conditions in practice – like extrusion – much better than the often used low scan rates, like 10 °C/min. Consistent with this awareness the window of analysis of the HyperDSC range of PerkinElmer has been enlarged up to cooling rates of 750 °C/min by way of the recently introduced DSC 8500.

Not only is the sequence of crystallization important but also the crystallizability itself matters: PBT crystallizes at 173 °C while the PET studied here does not crystallize anymore at cooling rates of 225 °C/min and higher. One should consider

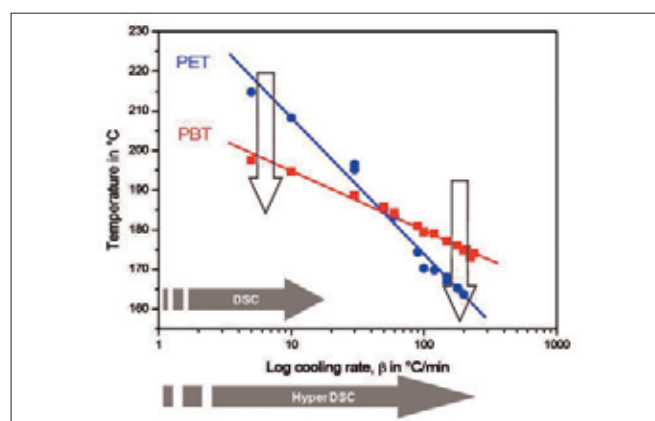


Figure 3. Crystallization temperatures of PET and PBT as a function of log cooling rate.

putting such “right” values into computer-aided industrial design software to improve polymer applications for automotive, shipbuilding, and aerospace industries, industrial and architectural design, prosthetics, and many more.

Thus, HyperDSC should be applied in order to mimic “real-life” processes and industrial processing much better than hitherto has been done. Furthermore, HyperDSC can handle sample masses ranging from approximately 1 µg or less up to more than 10 mg, by which one can choose a representative sample mass.

## Conclusions

Since polymer crystallization is significantly influenced by the actual cooling rate, the measurement of a characteristic crystallization temperature should be carried out at the same cooling rates as realized during polymer processing conditions. The conventional 10 °C/min cooling rate represents the low and small part of processing cooling rates applied in practice. Rates usually are much higher, near hundreds of degrees centigrade per minute. Therefore, results from a conventional cooling experiment using a scan rate of e.g. 10 °C/min can be misleading in practice, as illustrated by the PET and PBT case. Therefore, the fast cooling capability of HyperDSC is crucial for mimicking actual polymer processes – such as extrusion – and provides a realistic insight into polymer crystallization behavior. As such, it is an indispensable analytical tool to link experimental data with real-life polymer processes.

## References

1. Pijpers T.F.J., Mathot V.B.F., Goderis B., Scherrenberg R.L., van der Vegte E. *Macromolecules* 2002; 32:3601
2. Vanden Poel G., Mathot V.B.F. *Thermochim. Acta* 2006; 446:41.
3. Vanden Poel G., Mathot V.B.F. *Thermochim. Acta* 2007; 461:107.
4. V.B.F. Mathot, G. Vanden Poel and T.F.J. Pijpers, *American Laboratory*, 38(14) (2006) 21: downloadable for free from the website of SciTe B.V.: [www.scite.eu](http://www.scite.eu).

A special thanks to DSM Resolve and Science & Technology of the Netherlands for their contributions to this application note.

## Gas Chromatography

## Author

A. Tipler<sup>1</sup>PerkinElmer, Inc.  
Shelton, CT 06484 USA

## The Determination of C<sub>2</sub> to C<sub>5</sub> Hydrocarbons in Finished Gasolines using the PerkinElmer Clarus 680 GC with Swafer Technology

### Introduction

ASTM<sup>®</sup> Test Method, D2427-06, is designed to determine the C<sub>2</sub> to C<sub>5</sub> hydrocarbon content in gasolines. This method validates gasoline samples that are depentanized using ASTM<sup>®</sup> method D2001-07. These samples are intended for functional group hydrocarbon analysis by mass spectrometry according ASTM<sup>®</sup> Test Method D2789-95 (2005).

The method could be used for other sample types in which light aliphatic hydrocarbons are to be determined in samples containing significant low volatility or polar components in the matrix. The method is also suitable to determine methane content and could be extended to include higher hydrocarbons.

D2427-06 is a mature method that utilizes packed columns and mechanical valves for the backflush and foreflush techniques needed to separate the volatile hydrocarbons from the rest of the gasoline sample.

Modern gasolines contain significant concentrations of ethanol and other additives that may interfere with the existing method so there is a need to develop an alternative procedure to determine the light hydrocarbons. There have also been significant advances in column technology and chromatographic instrumentation that would improve the quality of the data and reduce the analysis time as well, so it would be appropriate to consider their use in this application.

<sup>1</sup> The author gratefully acknowledges the assistance of Rodrigo Favoreto, Daniel Santos and Fabio Boin of PerkinElmer, Sao Paulo, Brazil in the initial design and set up of this application work.

## Analytical Approach

An alumina porous layer open tubular (PLOT) column with split injection and flame ionization detection is for the separation of C<sub>2</sub> to C<sub>5</sub> saturated and unsaturated hydrocarbon isomers and is an obvious choice for this application. This column however will become easily 'poisoned' if higher hydrocarbons, aromatics or ethanol are allowed to pass into it. Thus, the analytical method will need to remove these compounds from the gasoline sample vapor before it enters the PLOT column.

The removal of these 'unwanted' components is easily achieved by deploying a 2-column backflushing system. A Carbowax® precolumn was chosen to enable the C<sub>2</sub> to C<sub>5</sub> hydrocarbons to elute and pass into the PLOT column before the higher hydrocarbons, aromatics or ethanol. Reversal of the direction of carrier gas flow in the precolumn, will back-flush the unwanted components back into the injector liner and out through the split vent. Chromatography of the C<sub>2</sub> to C<sub>5</sub> hydrocarbons will continue on the PLOT column during the backflush process. In this way, the backflush step does not add to the chromatographic run time.

Backflushing is a very effective technique for removing late-eluting unwanted material from a GC column.

## Experimental Conditions

The Swafer™ S6 configuration is used here with a fused silica restrictor tube on one of the outlet ports to enable the chromatography on the precolumn to be directly monitored by a detector. This enables the backflush point to be easily established.

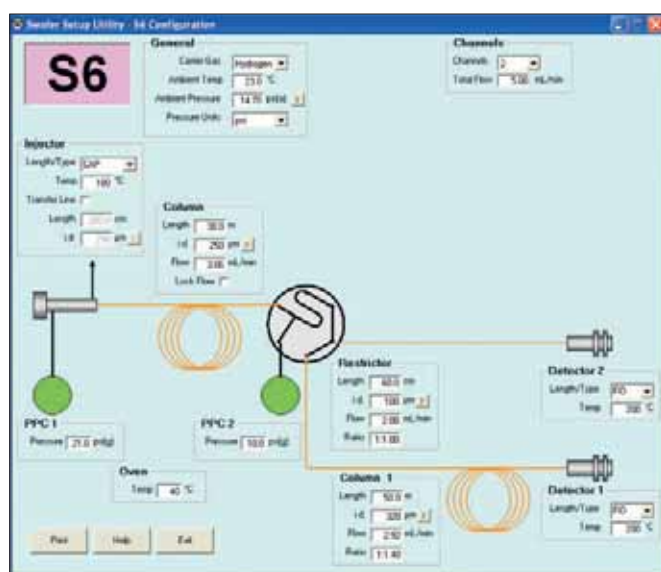


Figure 1. Swafer Utility Software showing the S6 configuration used in this method and gas pressures used for the initial work.

The Swafer Utility Software was used to establish the carrier gas pressures needed for this analysis. Figure 1 shows a screen shot taken from this software showing the configuration and suggested pressure settings used for the initial work.

Note that hydrogen is used as the carrier gas. This enables the run time to be reduced to increase sample throughput and eliminates the need for increasingly expensive helium as world stocks are depleting.

## Initial Method Set Up

To set up the system and identify and calibrate the target analytes, a refinery gas standard (RGS) was used as given in Table 1. Nearly all the target analytes listed in ASTM® D2427-06 are included and indicated in this mixture. The missing analytes are two methyl-butenes.

**Table 1. Arnel Refinery Gas Calibration Blend (Lot 102-06-04137, Cylinder # 10196D).**

Component	Mol%
Hydrogen	12.4819
Carbon Dioxide	2.9971
Ethylene*	2.0025
Ethane*	4.0021
Acetylene	0.9992
Oxygen	0.9998
Nitrogen	36.1691
Methane	5.0112
Carbon Monoxide	0.9984
Propane*	6.0185
Propylene*	3.0038
Isobutane*	5.0000
Propadiene*	0.9970
n-Butane*	3.9993
1-Butene*	1.9998
Isobutylene*	1.0025
t-2-Butene*	3.0061
c-2-Butene*	1.9996
1,3-Butadiene*	3.0107
Isopentane*	1.0009
n-Pentane*	2.0002
1-Pentene*	0.4007
t-2-Pentene*	0.1996
c-2-Pentene*	0.4001
2-Methyl-2-Butene*	0.1998
n-Hexane	0.1001

\* Target analyte listed in ASTM® D2427-06

50  $\mu$ L of the RGS gas mixture were injected by gas syringe with the restrictor from the Swafer connected to the detector as shown in Figure 2.

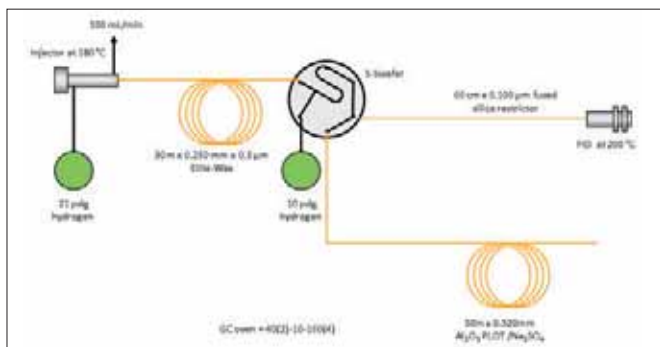


Figure 2. System configured to monitor the precolumn chromatography and establish the backflush point.

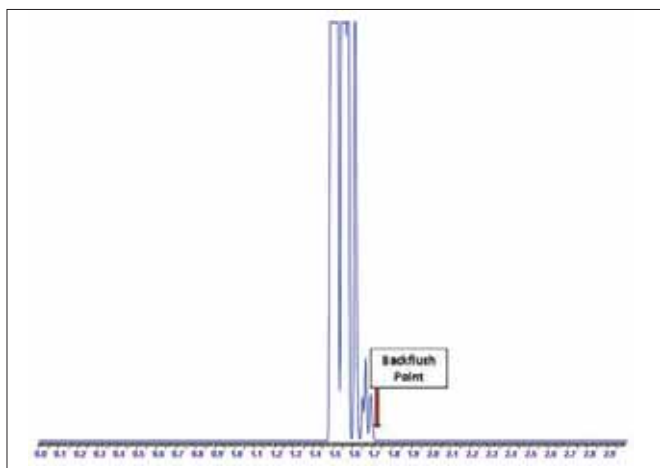


Figure 3. Precolumn chromatography of RGS mixture.

Figure 3 shows the resultant chromatography from this injection. All components have eluted from the precolumn (and into the PLOT column) within 1.7 minutes. To tolerate slight experimental variations, a backflush time of 1.72 minutes was adopted for the method.

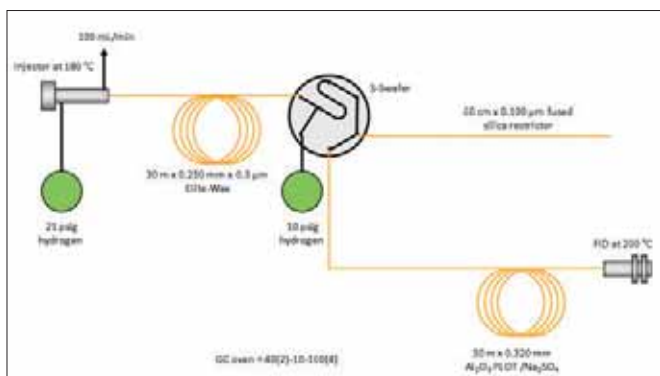


Figure 4. System configured to monitor the PLOT column chromatography to check the final chromatographic separation.

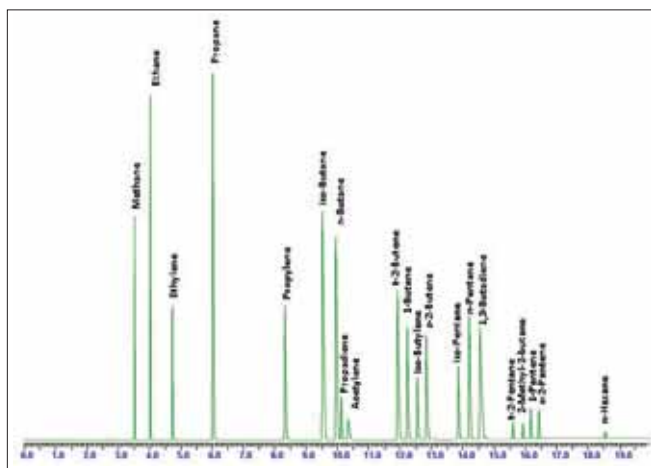


Figure 5. Chromatography of RGS mixture eluting from PLOT column.

To check the separation of the RGS mixture on the complete system, the restrictor was disconnected from the detector and the PLOT column was connected as shown in Figure 4 with a typical chromatogram given in Figure 5.

Study of Figure 3 and Figure 5 reveals that the precolumn chromatography finishes before the first peak (methane) elutes from the PLOT column. This means that both the restrictor and the PLOT column may be connected to the same detector to enable both the precolumn and PLOT column chromatography to be monitored in the same chromatogram.

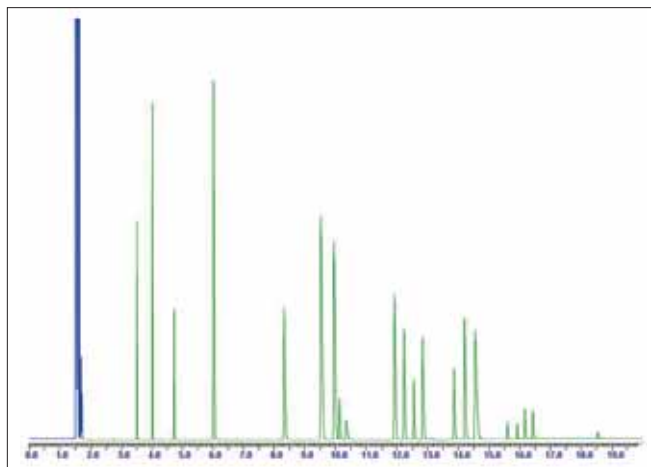


Figure 6. Combined precolumn and PLOT column chromatography of RGS mixture.

Figure 6 shows such a combined chromatogram. This approach makes set-up much easier as now there is no need to swap detector connections or buy an additional detector. The presence of both chromatograms in a single trace provides better QC as the precolumn chromatogram is now always present for checking.

When the pressure at the injector is reduced to initiate the backflush process, there is a time lag before the carrier gas starts to flow backwards into the precolumn from the Swafer. This means that sample material will continue to elute into the analytical column for several more seconds. To reduce this apparent time lag, a second timed event is added to the method to slightly raise the midpoint pressure inside the Swafer at the same time as reducing the inlet pressure.

The final method is given in Figure 7 and Table 2.

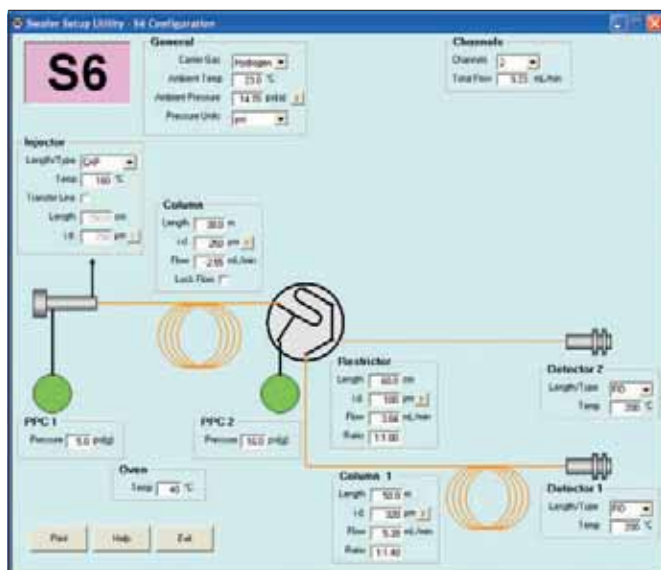


Figure 7. Screen shot taken from the Swafer Utility Software showing the system in backflush mode (note that in practice, a single detector is used).

<b>Table 2. Full experimental conditions.</b>	
Gas Chromatograph	PerkinElmer® Clarus® 680
Oven	40 °C for 2 minutes, then 10 °C/minute to 180 °C and hold for 5 minutes
Injector	Split/Splitless or Programmable Split/Splitless. 100 mL/min Split at 180 °C
Detector	Flame Ionization at 200 °C Air 450 mL/min, Hydrogen 45 mL/min Range x1, Attenuation x2
Backflush Device	S-Swafer in S6 configuration
Precolumn	30 m x 0.25 mm x 0.5 µm Elite Wax
Analytical Column	50 m x 0.32 mm Al <sub>2</sub> O <sub>3</sub> PLOT
Midpoint Restrictor	Fused silica, 60 cm x 0.100 mm
Carrier Gas	Hydrogen
Carrier Gas Pressure Programming	Inlet: 21 psig for 1.73 min, then 5 psig by timed event until end of run  Midpoint: 10 psig for 1.72 min then 16 psig by timed event until end of run (see text)
Injection	0.3 µL by Autosampler in fast mode

Figure 8 shows a chromatogram of the RGS mixture using the final conditions. Because the midpoint pressure has been raised for most of the run, the peak retention times are much shorter. Because the PLOT column retention relies on adsorption rather than partition, increasing the carrier gas pressure and hence the linear gas velocity does not significantly degrade column efficiency. In fact, the peaks shown in Figure 8 look better than those in the chromatogram in Figure 6 which was run at a lower midpoint pressure.

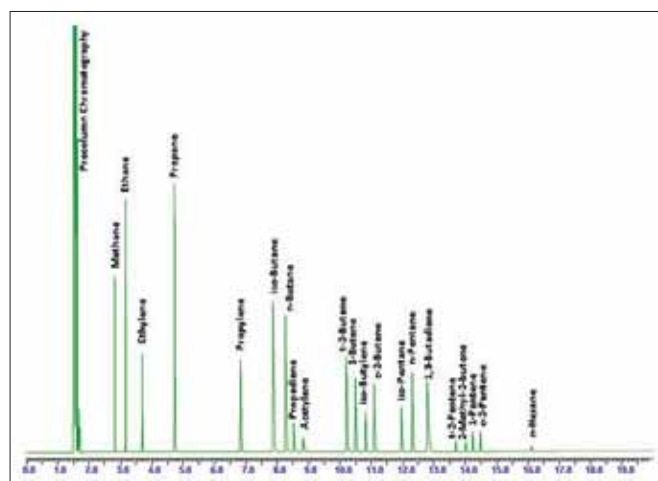


Figure 8. Chromatography of RGS mixture eluting from PLOT column with reduced inlet pressure and elevated midpoint pressure at backflush point.

Figure 9 shows a chromatogram of a gasoline sample run under these conditions.

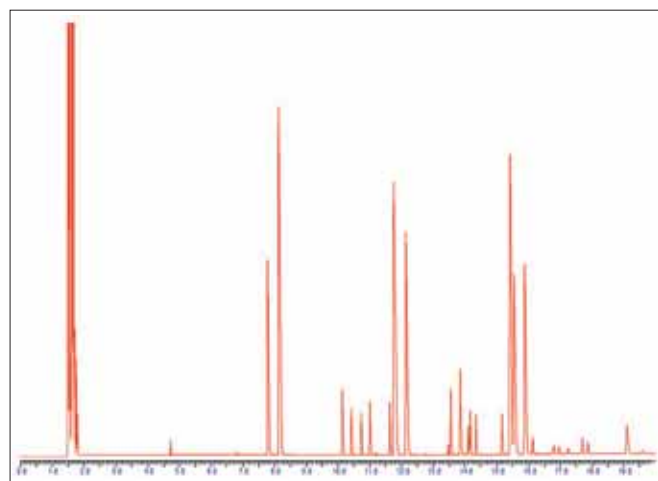


Figure 9. Combined precolumn and PLOT column chromatography with backflushing of a typical gasoline sample.

## Calibration

ASTM® Test Method, D2427-06 recommends the use of an internal standard such as 2-chloropropane for the quantitative calculations. Such compounds are not compatible with the alumina PLOT column and so external standard calculations were applied.

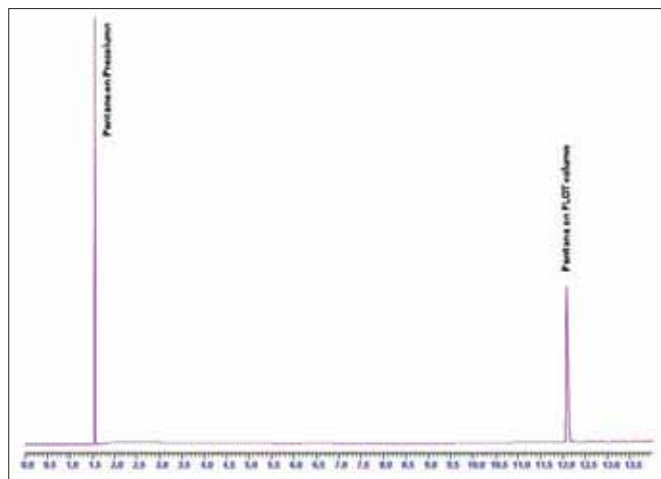


Figure 10. Chromatogram of 1.3% w/v solution of n-pentane in toluene.

The system was calibrated using a 1.3% w/v solution of n-pentane in toluene. The toluene is backflushed by the method and so only a peak for n-pentane appears as shown in Figure 10. The response factor calculation is shown in Table 3.

**Table 3. Calculation of response factor for n-pentane.**

Weight added (g)	0.1298
Diluted volume (mL)	10.0
Concentration (% w/v)	1.298
Peak area ( $\mu\text{V.s}$ )	974160
Response factor ( $\mu\text{V.s}/\%$ )	750508

Using the RGS mixture chromatography shown in Figure 8, peak areas were used to calculate relative response factors for the analytes as shown in Table 4.

These values were used to adjust the response factor of n-pentane given in Table 3 for application to each of the analytes. Note that n-pentane does not have to be in the sample for these calibrations to apply.

**Table 4. Response Factors calculated from RGS gas mixture.**

Component	Mol%	M.W	Peak Area $\mu\text{V.s}$	Response Factor Relative to n-Pentane (Area/wt.)	Absolute Response Factors ( $\mu\text{V.s}/\%$ )
Ethylene	2.0025	28	187178	1.14	855983
Ethane	4.0021	30	398308	1.13	850647
Propane	6.0185	44	877739	1.13	849893
Propylene	3.0038	42	421959	1.14	857610
Isobutane	5.0000	58	933182	1.10	825103
Propadiene	0.9970	38	127910	1.15	865697
n-Butane	3.9993	58	750601	1.11	829731
1-Butene	1.9998	56	368216	1.12	843078
Isobutylene	1.0025	56	175064	1.07	799586
t-2-Butene	3.0061	56	548315	1.11	835178
c-2-Butene	1.9996	56	358177	1.09	820176
1,3-Butadiene	3.0107	54	550241	1.16	867824
Isopentane	1.0009	72	219375	1.04	780557
n-Pentane	2.0002	72	421523	1.00	750508
1-Pentene	0.4007	70	82292	1.00	752283
t-2-Pentene	0.1996	70	41566	1.02	762808
c-2-Pentene	0.4001	70	82919	1.01	759151
2-Methyl-2-Butene	0.1998	70	39758	0.97	728905
3-Methyl-1-Butene	Absent	70	–	–	728905*
2-Methyl-1-Butene	Absent	70	–	–	728905*

\*Response factor assumed to be equivalent to 2-Methyl-2-Butene



## Example Analyses

Four samples of gasoline were obtained as listed in Table 5. These samples were of various vintages. The recent samples were known to contain ethanol whereas the earlier samples would contain MTBE. These should provide a good test for this method.

Sample	Description
1	2010 87-octane gasoline
2	Unleaded oxygen-free
3	1990 unleaded gasoline
4	2003 unleaded gasoline

To characterize these samples, each was chromatographed on the precolumn with no backflushing with just the precolumn connected to the detector. An example chromatogram is given in Figure 11. For the C<sub>2</sub> to C<sub>5</sub> determination, only the first 1.72 minutes of this pre-column chromatography will be sent to the PLOT column.

For the C<sub>2</sub> to C<sub>5</sub> determination, only the first 1.72 minutes of this precolumn chromatography will be sent to the PLOT column. It is clear that, with the backflushing method, all the aromatics, higher hydrocarbons and oxygenated compounds, including MTBE and ethanol, will be excluded from the PLOT column leading to a very rugged performance.

These same gasoline samples were now analyzed on the combined precolumn and PLOT column using the backflush method conditions given in Table 2. The resultant chromatograms are given in Figure 12.

The peak areas from the chromatograms shown in Figure 12 were processed using the response factors given in Table 4.

To check the quantitative precision, one of the gasoline samples was injected 10 times and the standard deviations were calculated for the quantitative results and the peak retention times, are shown in Table 7. These results far exceed the requirements of method D2427.

Component	Sample 1	Sample 2	Sample 3	Sample 4
Ethylene	N.D.	N.D.	N.D.	N.D.
Ethane	N.D.	N.D.	N.D.	N.D.
Propane	N.D.	N.D.	N.D.	0.05
Propylene	N.D.	N.D.	N.D.	0.01
iso-Butane	0.06	0.19	0.01	1.66
Propadiene	N.D.	N.D.	N.D.	N.D.
n-Butane	0.61	1.36	0.06	3.68
1-Butene	N.D.	0.04	N.D.	0.26
iso-Butylene	N.D.	0.04	N.D.	0.25
t-2-Butene	0.01	0.17	0.01	0.41
c-2-Butene	0.02	0.19	0.02	0.33
1,3-Butadiene	N.D.	N.D.	N.D.	N.D.
iso-Pentane	3.33	4.54	4.18	3.64
n-Pentane	1.62	1.54	2.60	2.36
1-Pentene	0.10	0.36	0.15	0.15
t-2-Pentene	0.42	0.96	0.38	0.43
c-2-Pentene	0.19	0.53	0.22	0.23
2-Methyl-2-Butene	0.67	1.33	0.67	0.64
3-Methyl-1-Butene	0.03	0.11	0.06	0.05
2-Methyl-1-Butene	0.26	0.66	0.32	0.29
<i>N.D.: None Detected</i>				

Component	Concentration		
	Mean (% w/v)	Std Dev (% w/v)	D2427-06 Req. (% w/v)
Ethylene	N.D.	N.D.	
Ethane	N.D.	N.D.	
Propane	0.04	0.0002	0.1
Propylene	N.D.	N.D.	0.1
iso-Butane	1.62	0.0105	0.1
Propadiene	N.D.	N.D.	
n-Butane	3.59	0.0174	0.1
1-Butene	N.D.	N.D.	0.1
iso-Butylene	0.25	0.0026	0.1
t-2-Butene	0.40	0.0023	0.1
c-2-Butene	0.32	0.0019	0.1
1,3-Butadiene	0.00	0.0000	
iso-Pentane	3.58	0.0245	0.3
n-Pentane	2.33	0.0170	0.1
1-Pentene	0.15	0.0013	0.1
t-2-Pentene	0.42	0.0036	0.1
c-2-Pentene	0.23	0.0020	0.1
2-Methyl-2-Butene	0.64	0.0063	0.3
3-Methyl-1-Butene	0.05	0.0004	
2-Methyl-1-Butene	0.28	0.0027	0.2
<i>N.D.: None Detected</i>			

## Other Sample Types

Although this method was primarily designed to determine light hydrocarbons in finished gasolines, it can be applied to any sample in which there are significant levels of less volatile or more polar components in the matrix.

Figure 13 shows an example of chromatography from an injection of a light crude oil using this method. The method was modified slightly by increasing the injector temperature to 250 °C to assist in the volatilization of the heavier sample. Note that none of the heavy hydrocarbons in the crude oil were able to enter the PLOT column.

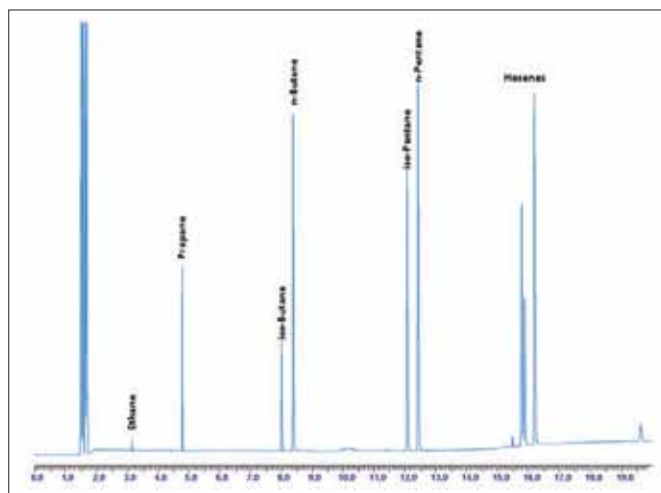


Figure 13. System chromatogram of a sample of light crude oil diluted 50:50 with toluene.

## Conclusions

- The combination of modern capillary columns with the Swafer technology has taken a mature method and improved the quality of the data and reduced the run time as intended.
- Excellent separation of the C<sub>2</sub> to C<sub>5</sub> aliphatic hydrocarbons is evident with no apparent interference from higher hydrocarbons, aromatics or oxygenated compounds.
- Even though the method relies on significant carrier gas pressure and flow rate changes, the quantitative and peak retention time precisions are excellent.
- The chromatographic run time has been reduced from over 60 minutes to just 20 minutes. The total cycle time of the chromatographic analysis (including oven cool-down and equilibration) is less than 24 minutes enabling 20 samples to be analyzed during an 8-hour working shift or 60 samples a day if run continuously.
- The method will also determine levels of methane, if present (in other sample matrices).
- The method would be suitable for the analysis of other sample types in which volatile aliphatic hydrocarbons are to be monitored in a matrix containing higher hydrocarbons, aromatics and/or polar components.
- The method could be extended to allow the determination of higher hydrocarbons by increasing the time of the backflush point.

## FT-IR Spectroscopy

**Authors:**

Enrique Lozano Diz

Richard Spragg

PerkinElmer, Inc.  
Seer Green, UK

## Analysis of UV-Curable Resins by FT-IR

### Introduction

There are on the market an increasing number of special adhesives, coatings and sealants that allow curing in just few seconds upon exposure of the resin to the appropriate radiation. Those adhesives are gaining great interest in specialized applications (medical, glass and lighting repairs, rapid prototyping, etc.) because they allow accurate and immediate bonding and avoid some of the more problematic aspects like toxicity, polluting and organic solvent formulations of conventional adhesives.

Typically these resins cure by using UV and, more recently, visible radiation to initiate a photochemical reaction that proceeds to the curing of the resin. Many parameters may affect the speed and depth of the curing, including the intensity of the illumination, the spectral range used during the curing (single wavelength or range of wavelengths), thickness of the curing area, distance to the light source, transparency of the substrate the light must pass through, and many other environmental parameters, such as nature of the material to bond and presence of external oxidizing materials, that affect the time of hardening the adhesive.

It is important to have a good understanding not just of the speed of cure but also of the mechanism of the curing process. One way to investigate and quantify the curing process is to measure spectroscopic changes of the functional groups involved in curing. The formation and destruction of functional groups is easily followed by rapid scan FT-IR. Determining relative peak areas can help to understand the kinetics process and identifying the presence of reaction intermediates can help to understand how changing conditions affect the curing process.

Many photo-curable adhesives, coatings and sealants are based on acrylates. The curing process involves a photo-initiator that forms free radicals when exposed to UV radiation. The radicals react with acrylate monomers, opening the double bonds to form further radicals. These react with further acrylate molecules, building up chains with cross-linking to provide a network that gives mechanical strength to the cured product. The kinetics of the curing process depends on the generation of the reaction intermediates, so their detection, characterization and quantification are fundamental to understanding the properties of a resin.

### Monitoring the reaction

Numerous techniques have been used to study the curing process. Differential scanning calorimetry (DSC) measures the heat produced by the reaction and so can determine the degree of cure as the reaction proceeds. Dynamic mechanical analysis (DMA) measures the modulus of the resin so that the properties of the cured material can be related to the degree of cure. FT-IR spectroscopy provides more chemical information than DSC because many absorption bands are measured. For example in an acrylic resin the curing process involves the disappearance of C=CH<sub>2</sub> groups in the monomer. The progress of this can be followed by measuring the intensity of absorption bands that are specifically associated with these groups, such as the C=CH<sub>2</sub> twisting at 812 cm<sup>-1</sup> or the =CH<sub>2</sub> deformation near 1400 cm<sup>-1</sup>. No bands are completely free from overlap which hinders kinetic analysis but qualitative measurements are straightforward. Figure 4 shows the decay in absorbance of the 812 cm<sup>-1</sup> band for two different UV intensities. However disruption of the double bond is only the first step in the reaction as radicals produced by photoinitiation react with acrylate groups and cross-linking proceeds.

An overview of the reaction is obtained by applying principal components analysis (PCA) to the data. For a simple reaction there should be a single principal component representing the difference in spectra between the starting material and the product. For the resin studied here we consistently find two principal components. The first PC accounts for about 99% of the variance while the second PC accounts for the remaining variance except noise. The scores for the first PC correspond to the overall reaction, changing monotonically, but the scores for the second PC



Figure 1. Frontier spectrometer with ATR accessory.

reach a peak during the most rapid phase of the reaction Figure 5. Thus the second PC can provide information about the intermediate stage of the reaction that is not available from DSC measurements.

### Experimental

Spectra were measured with a Frontier™ FT-IR spectrometer, a research grade instrument with fast scanning, collecting up to 16 scans/second which is more than sufficient to follow reactions with half-lives of a few seconds. Data collection was controlled using PerkinElmer® TimeBase™ software. The same software can generate profiles of specific band intensities or intensity ratios as a function of time. Data were also analyzed with Principal Components Analysis (PCA) using the QUANT+ program.

The most convenient approach to making these measurements is to use a diamond ATR accessory. The liquid resin is placed on the diamond crystal and illuminated from above. We used a UATR accessory with a single-bounce diamond crystal (Figure 1). The UV source was an Omnicure® S2000 and fiber-optic light guide with variable output, providing radiation from 320 to 500 nm.

The resin was Loctite® 3494, a clear light cure adhesive used for bonding glass and plastics.<sup>1</sup> It contains a mixture of acrylate and methacrylate monomers with a benzoyl phosphine oxide initiator. We verified that curing was extremely slow under the background laboratory illumination.

A drop of resin was placed on the crystal and the UV illumination was switched on a few seconds after starting data collection. Spectra were recorded with 16 scans/second. Two illumination levels were used, 10 and 50% of the maximum, corresponding to outputs of 75 and 430 mW at 365 nm.

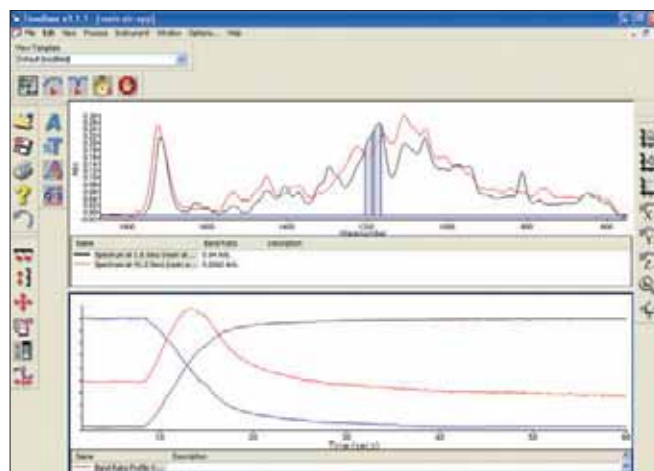


Figure 2. Typical TimeBase screen with intensity profiles from resin curing.

## Results

Spectra of the initial and fully cured resins are seen in Figure 3. Typical intensity profiles derived from the  $=CH_2$  twisting vibration at  $812\text{ cm}^{-1}$  are shown in Figure 4. The profiles are taken from 800 scans obtained in 50 seconds. The reaction is much faster with the higher illumination level, being nearly complete after 10 seconds.

The results from PCA for the two illumination levels are seen in Figure 5. Clearly they show the same pattern, the scores on PC2 peaking in both cases at the time that scores on PC1 are changing most rapidly.

## Discussion

These data clearly show the suitability of the Frontier spectrometer with TimeBase software for studying the UV curing process. PCA demonstrates that the data contain more information than can be obtained from UV-DSC measurements as an intermediate process is revealed. The complexity of this commercial formulation makes interpretation difficult but investigation of simpler systems would be feasible.

Using ATR is very convenient and allows UV illumination without an intervening window. One limitation is that curing is being measured only for the layer in contact with the crystal. In this case the amount of the resin as uncontrolled but curing at different depths can be studied by varying the thickness of the resin layer.

## Reference

1. Henkel Ltd., Hemel Hempstead, England.

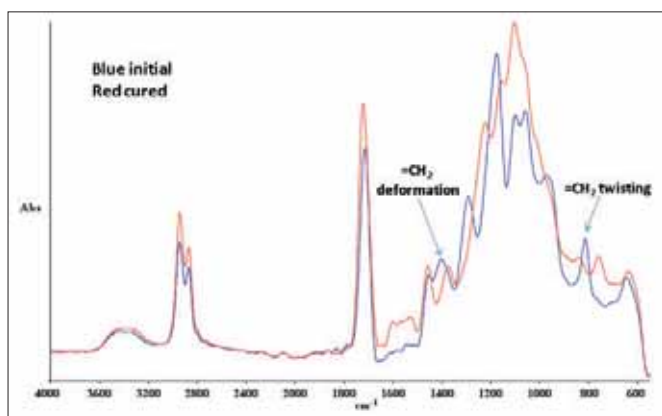


Figure 3. ATR spectra of Loctite® 3494 resin before and after curing.

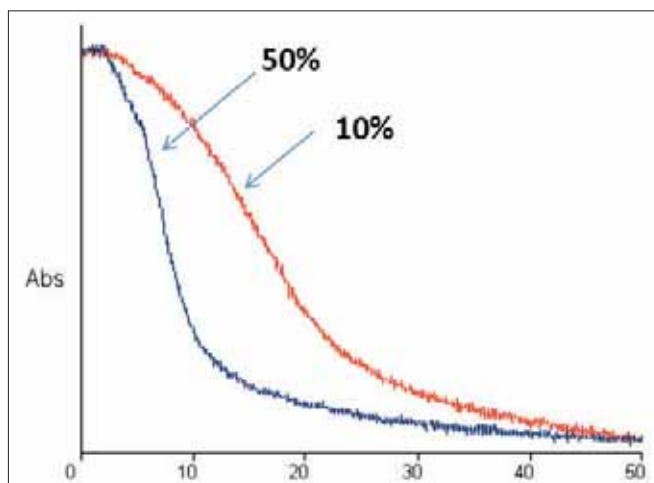


Figure 4. Intensity profiles of the  $=CH_2$  twisting band at  $812\text{ cm}^{-1}$  for different illumination levels.

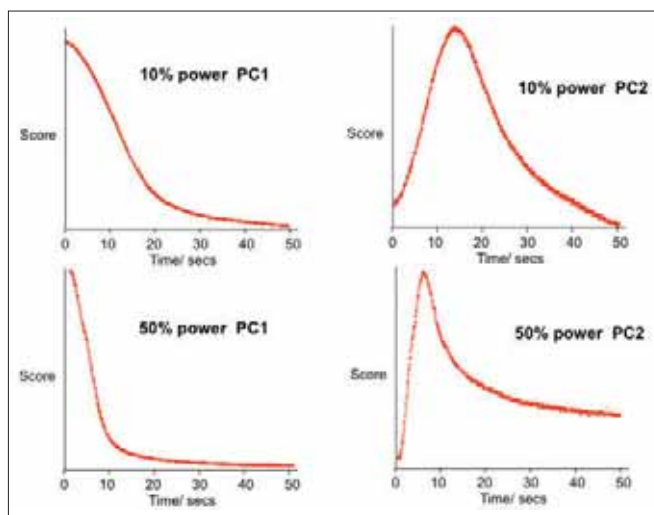


Figure 5. Principal component scores for resin curing at different illumination levels.

## FT-IR Spectroscopy



## Cavity-enhanced Absorption Spectroscopy for Trace Gas Detection with Frontier

### Introduction

Detecting gases at low concentrations with FT-IR requires long pathlengths to increase absorption. The conventional approach employs a multi-pass White Cell where the light beam is reflected between two mirrors that are angled so that the beam emerges past one of the mirrors after a number of reflections, giving pathlengths up to tens of meters. In cavity-enhanced measurements, a highly collimated beam is reflected between two mirrors with a small amount of radiation emerging through the mirrors at each reflection. By using highly reflective mirrors the effective pathlength can be several thousand times greater than the separation between the mirrors. This gives the possibility of detecting gases at low concentrations in relatively small volumes, for example in looking for metabolites in breath.

Cavity-enhanced absorption spectroscopy (CEAS) has similarities with the better known cavity ringdown technique (CRDS) which measures the signal decay as a laser pulse emerges through one of the mirrors after successive reflections. By measuring the increase in the rate of decay caused by an absorbing species, CRDS can measure ppb concentrations of small molecules. The ringdown technique has typically been applied to small molecules where the wavelength of a NIR laser source can be tuned across very narrow individual lines of the spectra. In contrast this report describes CEAS using a broadband source applied to larger molecules where the spectra are broader.

The measured signal is the sum of light that has passed through the cavity different numbers of times. Figure 1 shows that fraction of light transmitted as a function of the number of reflections for different reflectivities. The reflectivity of the mirrors is typically greater than 99.95% so that a significant fraction of the light undergoes thousands of reflections. When the separation between the mirrors is  $L$  and the reflectivity is  $R$  the effective pathlength is  $L/(1-R)$ . For a 25 cm separation and reflectivity of 0.9995 the effective pathlength is 500 meters. Because there is no single pathlength the Beer-Lambert law does not apply. Instead the relationship between concentration,  $C$ , and incident and transmitted intensities,  $I_0$  and  $I$ , is given by:  $C \propto (I_0 - I) / I$ .<sup>1</sup>

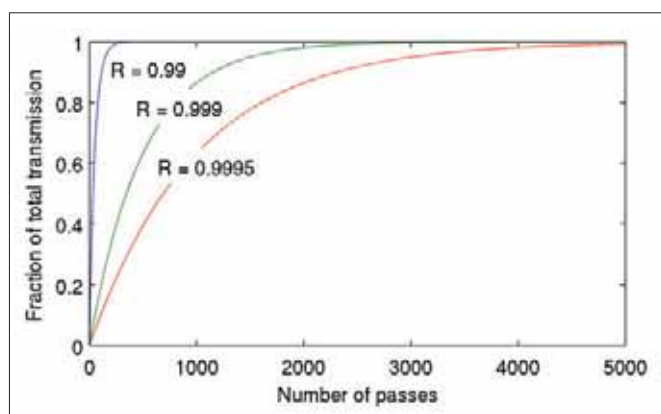


Figure 1. The fraction of intensity transmitted vs. the number of passes.

The high reflectivity of the mirrors means that only a very small fraction of the source radiation enters the cavity. For this reason laser sources have generally been used. The work described here was aimed at reducing the cost and complexity of the technique by using a near IR superluminescent diode (SLED) as the light source.<sup>2</sup>

## Experimental

The light source was a fiber-coupled SLED with an output of 10 mW centered at  $6000 \text{ cm}^{-1}$  and bandwidth approaching  $400 \text{ cm}^{-1}$ . The cavity was positioned between the source and the emission port of a near IR Frontier™ fitted with an InGaAs detector. Aligning the system proved far easier than when using a monochromator because of the large circular aperture of the spectrometer. The principal target species was 1,3-butadiene, which is a common hazardous air pollutant. Spectra were measured at 4 or  $16 \text{ cm}^{-1}$  resolution. The cavity length was 25 cm and mirror reflectivity was measured to be up to 99.98%. This gives a pathlength enhancement factor of 5000 resulting in an effective pathlength of 1.25 km. A schematic of the system is shown in Figure 2.

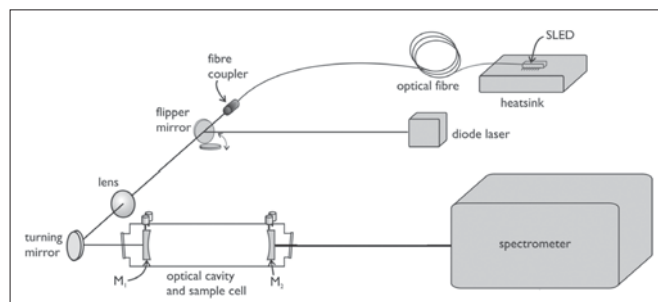


Figure 2. Schematic of experimental setup.

## Results

Spectra were measured at resolutions between  $0.5$  and  $16 \text{ cm}^{-1}$ . As the bands in the spectrum of 1,3-butadiene are relatively broad a resolution of  $16 \text{ cm}^{-1}$  is sufficient. Figure 3 shows cavity-enhanced spectra of butadiene at concentrations between 300 and 80 ppm. From separate measurements of the scan-to-scan noise the detection limit for 1,3-butadiene for a four minute measurement is estimated to be about 600 ppb.

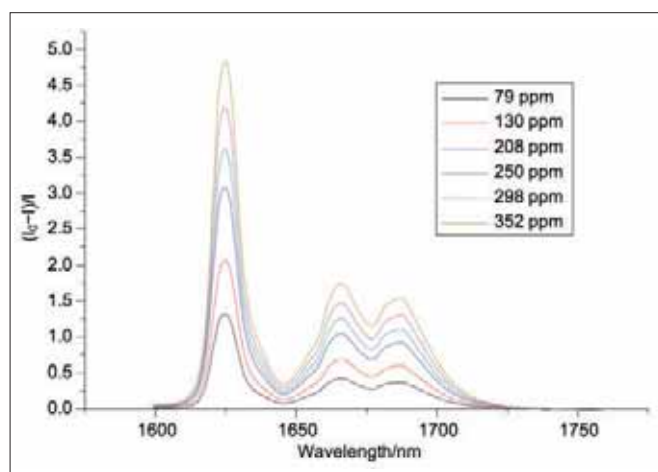


Figure 3. Spectra of 1,3-butadiene.

One of the principal attractions of cavity enhanced spectroscopy is the possibility to observe multiple species. Figure 4 shows spectra of isoprene, methane and a mixture containing 10 ppm methane and 120 ppm isoprene in air. At  $4 \text{ cm}^{-1}$  resolution, the fine structure of the methane spectrum can be seen superimposed on the broad bands of isoprene.

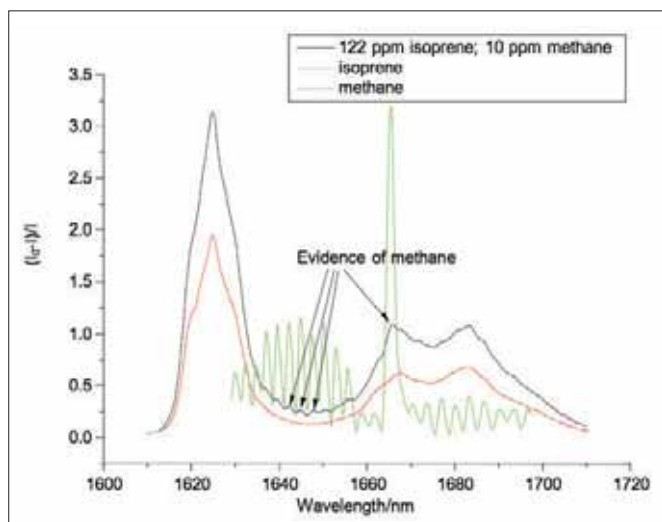


Figure 4. Spectra of isoprene (red), methane (green) and a mixture with 10 ppm methane and 120 ppm isoprene in air.

## Summary

Cavity-enhanced absorption measurements with a SLED source and Frontier with an InGaAs detector can achieve ppm sensitivity for measuring 1,3-butadiene. Other hydrocarbon species have been measured with the same system. The spectral range can be increased by multiplexing SLED's but the very high reflectivities needed cannot be maintained over a wide spectral range.

## Acknowledgment

The CEAS/SLED technology described here has been developed in the Physical and Theoretical Chemistry Laboratory (Oxford University) and will be exploited for medical and other commercial applications by Oxford Medical Diagnostics, Ltd.

## References

1. M. Mazurenca, A.J. Orr-Ewing, R. Peverall, G.A. Ritchie, *Annu. Rep. Prog. Chem. Sect. C*, 2005, **101**, 100-142.
2. W. Denzer, M.L. Hamilton, G. Hancock, M. Islam, C.E. Langley, R. Peverall and G.A.D. Ritchie, *Analyst*, 2009, **134**, 2220-2223.

PerkinElmer, Inc.  
940 Winter Street  
Waltham, MA 02451 USA  
P: (800) 762-4000 or  
(+1) 203-925-4602  
[www.perkinelmer.com](http://www.perkinelmer.com)



For a complete listing of our global offices, visit [www.perkinelmer.com/ContactUs](http://www.perkinelmer.com/ContactUs)

Copyright © 2011, PerkinElmer, Inc. All rights reserved. PerkinElmer® is a registered trademark of PerkinElmer, Inc. All other trademarks are the property of their respective owners.

009261\_01

## Differential Scanning Calorimetry

## Authors

James Outlaw  
Champion Technologies  
Fresno, TX 77545

Peng Ye  
PerkinElmer, Inc.  
Shelton, CT 06484 USA

## Wax Appearance Temperature Detection by DSC

### Introduction

Crude oils and natural gas fluids are composed of nearly 100% hydrocarbons. A series of naturally occurring hydrocarbons with the chemical formula  $C_nH_{2n+2}$  are known as paraffins. In most crude oils, the paraffins align as long straight chain molecules. However, they can also form branched or cyclic structures. A collection of normal paraffins, with 16 or more carbon atoms ( $\geq C_{16}$ ) that form crystalline solid substances at 68 °F (20 °C), are known as wax. The amount of wax contained in a crude oil sample varies, depending on the geographic source of the crude. Whenever the temperature decreases the dispersed paraffins begin to align together. As cooling of the crude oil continues, the paraffins form a solid crystalline wax structure. The crystal growth produces high molecular weight wax, which reaches a point where it precipitates out of the crude oil. In clear crudes the wax deposition gives the oil a cloudy appearance. This temperature is called the cloud point, or wax appearance temperature (WAT).

Since paraffins and wax occur naturally in crude oil, there is a potential for wax deposition at every step from oil production to refining. The wax deposits reduce the internal diameter of tubular transportation pipelines, restrict or block valves, and impede other production equipment. Severe wax deposition can lead to a complete stop in production; which can translate into millions of lost dollars in sales. There are many ways to remove or prevent wax deposition. For example, thermal methods include heating and insulating the pipeline or introducing hot fluids above the WAT to melt or prevent wax deposition. A wax crystal modifier can be added to the oil to prevent the wax deposition even below the WAT. However, for these two methods, their effectiveness is dependent upon the WAT.

WAT can be determined according to ASTM® D2500. In this method, the starting transparent sample oil is poured into a test jar. A thermometer is used to monitor the oil temperature. The entire jar is then put into a constant temperature bath. The cooling bath temperature is reduced by 1 °C step by step and the sample oil is examined visually through a microscope for crystal formation. The WAT is determined as the temperature at which the crystals first appear. This method is quite time-consuming and is not automatic – it needs the operator interaction. Another method for WAT determination is using differential scanning calorimetry (DSC). DSC measures the heat flow from or to the sample when the sample is heated or cooled. Since crystallization will give out heat, it will show up in the DSC curve as an exothermic peak during cooling. Only a small amount of sample oil is needed for DSC analysis. Since it utilizes heat to detect the onset of wax crystallization the sample doesn't need to be transparent, it can even be dark. With an autosampler, many samples can be run automatically without operator's interaction.

So DSC is an effective tool to characterize the WAT for the oil industry. It is also useful to optimize chemical treatment parameters for cost-effective wax control, including selecting optimal wax crystal modifier and treatment formulation. In this paper, the Diamond DSC from PerkinElmer is used to determine the WAT of an oil sample.

## Experiment

Once a sample of crude oil or a wax deposit is received from the well site, it is prepared for analysis. Figure 1 shows the crude oil sample above WAT on the left and crude oil sample below WAT on the right. After transferring the sample into a thermally safe container, the crude oil is heated in an oven at 80 °C for 2 hours. This will ensure that the suspended waxes will be melted. Once the crude oil is thoroughly heated, a 30 micro-liter sample is injected into the DSC stainless steel hermetic pan (Figure 2). The o-ring and lid are inserted on top of the pan and compressed to form a seal.

The hermetically-sealed pan will prevent any evaporation of oil at high temperature. The temperature parameters are set for a typical maximum temperature of 120 °C to a minimum of -20 °C at a rate of 10 °C/minute in the Pyris™ Player.

The instrument used here is the Diamond DSC from PerkinElmer with an autosampler (Figure 3). The Diamond DSC features the proprietary double furnace power compensation design. It offers highly sensitive and accurate temperature and heat flow measurement.



Figure 1. Crude oil sample above WAT (left) and crude oil sample below WAT (right).



Figure 2. Stainless steel pan (Part Number 03190218) used for this experiment.



Figure 3. Diamond DSC with autosampler.

## Results

Once the DSC has completed the test, a graph will be produced. It will require the operator to take a more in depth look in order to find the desired information. As the oil sample is cooled from the maximum temperature, the heat trace measures the energy at each temperature. Once the paraffins align themselves and begin to form crystals, energy in the form of heat is given off. The exothermic reaction of crystallization is recorded. This temperature is determined to be the wax appearance temperature (WAT).

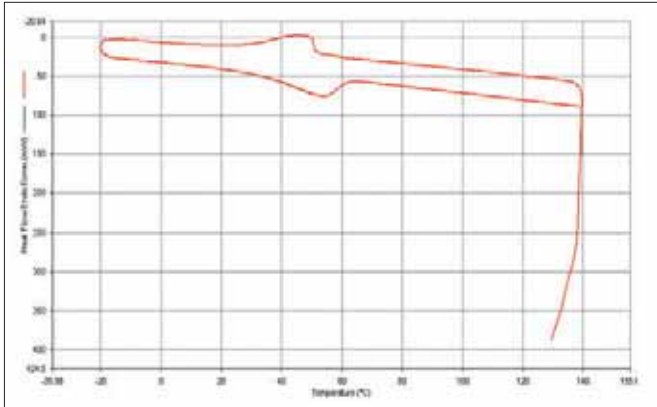


Figure 4. DSC Heat Flow curve.

In order to locate the wax appearance temperature, only the cool down portion of the Heat Flow curve is selected. It will allow for magnified viewing of the curve, as well as additional analysis.

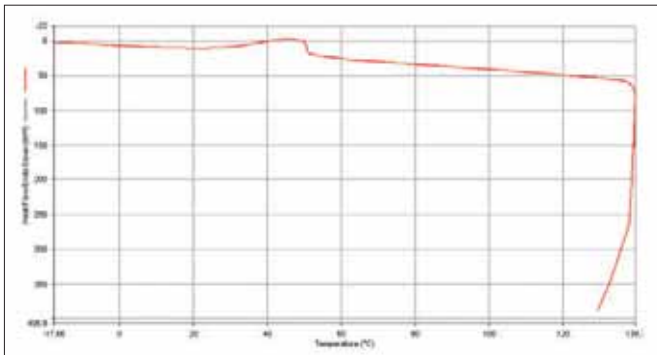


Figure 5. Heat Flow Cool Down curve selected view.

In many cases, the change in slope is not easily detected on the Heat Flow Cool Down curve. By looking at the derivative plot of the curve, we are able to zoom in on the defined exothermic peak of the curve.

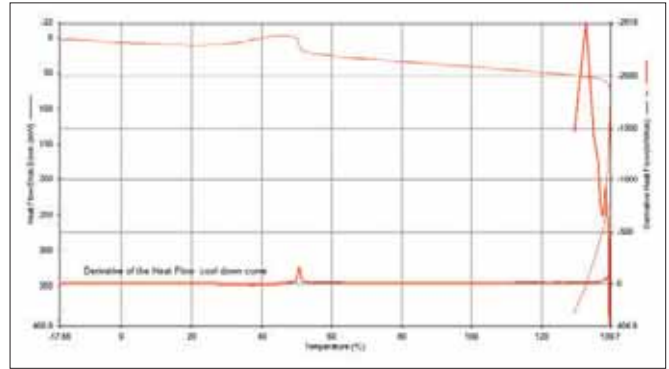


Figure 6. Derivative curve of the Heat Flow Cool Down curve.

After magnifying the derivative curve, the Onset temperature is ready to be calculated. The Onset temperature is denoted by the section of the curve where the heat flow begins to decrease as the oil sample gives off heat energy.

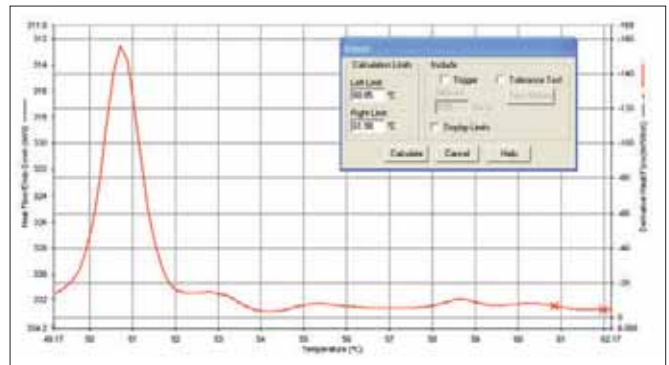


Figure 7. Onset calculation using the derivative curve.

The Onset temperature is calculated by adjusting the lines to find the tangent point where the slope changes. The calculated temperature will be noted as the Wax Appearance Temperature.

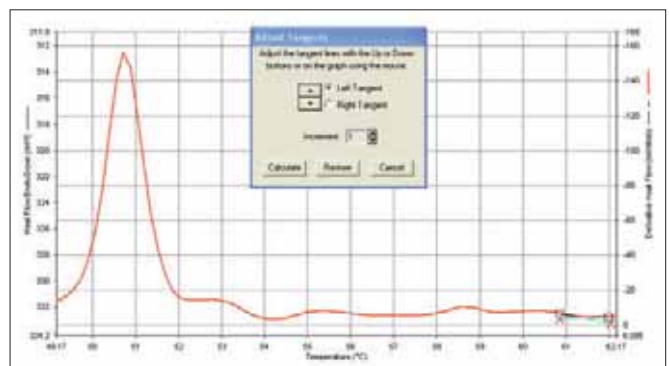


Figure 8. Adjustment of tangent arms in order to calculate the onset.

The recorded temperature of the Onset temperature will be denoted on the Heat Flow curve.

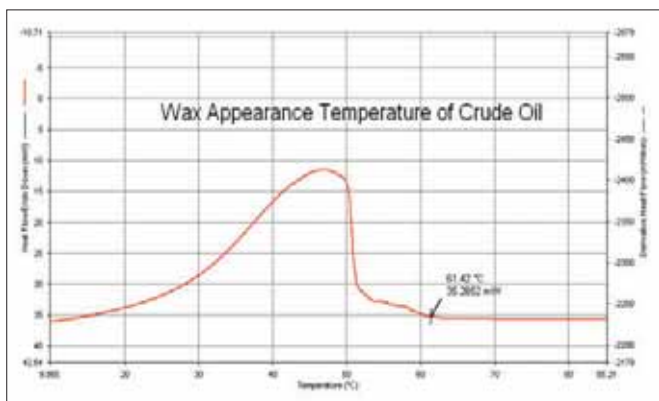


Figure 9. Notation of wax appearance temperature on Heat Flow Cool Down curve.

## Conclusion

The DSC is a very important tool for the oil field industry. Its capabilities allow for the measurement of the Wax Appearance Temperature, which is used to predict and prevent the occurrence of wax deposition. The DSC's ease of use, multi-sample capability, and powerful analysis software make it an ideal measurement tool.

## FT-IR Spectroscopy

Author:

Enrique Lozano Diz

Richard Spragg

PerkinElmer, Inc.  
Seer Green, UK

## Investigating Phase Transitions with Variable Temperature ATR

### Introduction

Heating and cooling cause phase changes in many materials with consequent effects on their physical properties. IR spectroscopy is a powerful tool for studying these changes since the spectra are sensitive to variations in both intermolecular and intramolecular interactions. Changes in the IR spectra due to temperature variations can be correlated with structural changes and the spectra

can be associated with specific crystalline forms. For example, any transition from a crystalline to an amorphous phase results in a broadening of bands as the molecules are in more varied environments. In crystalline materials, a change from one polymorph to another generally causes band shifts and splitting. For many materials transmission and external reflection measurements are not practicable without some sample preparation but ATR can often be used directly. In this note we illustrate the use of heated ATR to follow thermal changes in chocolate, which is largely a suspension of sucrose and cocoa solids in a matrix of cocoa butter. Chocolate and cocoa butter both have several polymorphs with melting points between 17 and 37 °C.<sup>1</sup> The polymorphic form has to be carefully controlled in manufacture because of its importance for storage and its major contribution to the sensory experience when eating chocolate.

## Experimental

Spectra were measured with a Frontier FT-IR spectrometer using a single bounce PIKE ATR accessory with a ZnSe crystal that could be heated at a controlled rate up to 135 °C. The heating rate was usually 1 degree C/minute with 4 cm<sup>-1</sup> spectra collected at 15 second intervals using PerkinElmer® TimeBase™ software (Figure 1). The materials used were cocoa butter and a commercial dark chocolate product containing 85% cocoa and about 15% sucrose with other minor constituents.<sup>2</sup>

## Results

Caution is needed in interpreting ATR spectra because they come from the first few microns depth of material in contact with the crystal. Because of this, ATR spectra may differ from those of the bulk material. The penetration depth is proportional to wavelength which means that relative band intensities in different regions may change if the degree of contact with the crystal changes. In this case the bands used to generate band ratios were separated by less than 20 cm<sup>-1</sup> so the difference in penetration depth is insignificant.

Typical ATR spectra of chocolate and cocoa butter are shown in Figure 2. The chocolate spectrum is dominated by the cocoa butter which is largely a mixture of di and triglycerides of stearic, palmitic and oleic acids, and by sucrose. As the sample is heated (Figure 3) the features associated with cocoa butter broaden and shift while the sucrose bands are unchanged. Melting causes an overall increase in band intensities because of improved contact with the ATR crystal. At the same time there is a reduction in the intensities of all the sucrose bands relative to those of the cocoa butter. This is attributed to the liquid cocoa butter flowing around the sucrose crystals on to the surface of the crystal.

Although there are changes occurring in many regions of the spectra they are seen most clearly in the complex C=O absorption around 1740 cm<sup>-1</sup>. The C=O feature of three samples of the same chocolate with different thermal histories at about 20 °C are seen in Figure 4. Three peaks are seen in the original material but their relative intensities are affected by heating and cooling. After melting and cooling there is a broad unresolved band. The changes with temperature can be followed by monitoring appropriate band intensities within this region or, in more detail by using principal components analysis (PCA).

TimeBase software provides several different ways of presenting the data, as individual spectra or a stacked plot. The changes with temperature can be examined as the

intensities at specific frequencies or as ratios of pairs of peak heights or band areas that can be chosen interactively. The use of band intensity ratios is especially appropriate for ATR data as the overall intensities can be affected by changes in the contact with the ATR crystal. Figure 5 shows typical TimeBase screen displays.

In Figure 6 the ratio of intensities at different frequencies within the C=O band for chocolate is compared with the same ratio for a cocoa butter as each is heated to above its melting point. There appears to be a single smooth transition for cocoa butter while the chocolate melting appears more complex. PCA of the chocolate spectra identifies several significant principal components. Combinations of the scores for the first two PC's separate one process that appears complete at 25 °C from a second that occurs between 25 and 30 °C (Figure 7). Identifying the specific polymorph changes associated with these transitions would require reference spectra of the individual polymorphs which were not available at the time of this study.

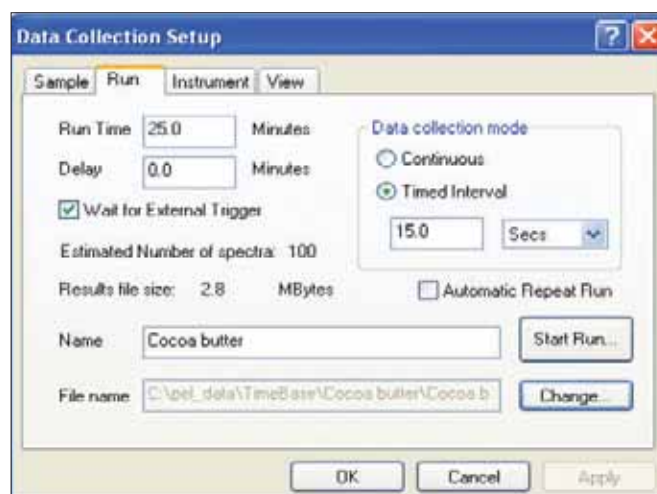


Figure 1. Set-up screen for TimeBase.

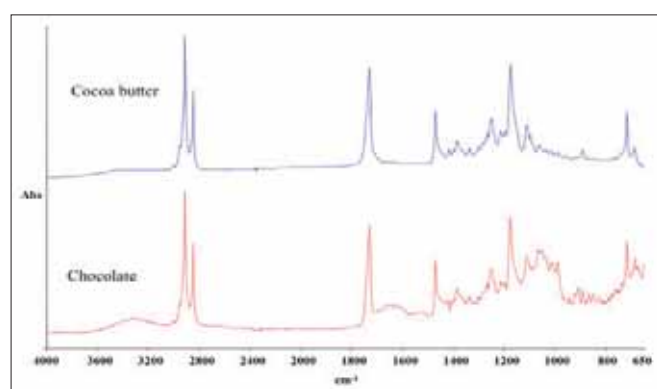


Figure 2. Spectra of chocolate and cocoa butter.

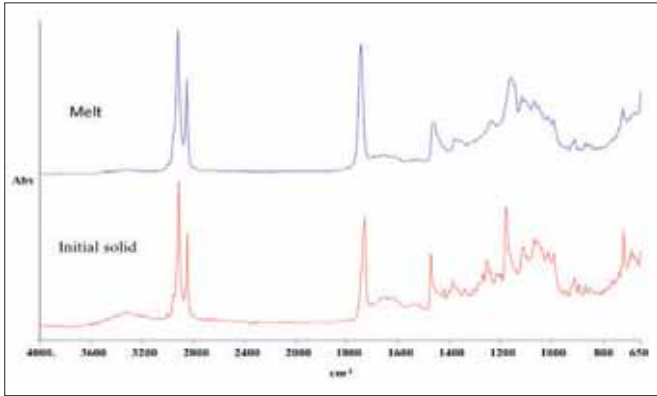


Figure 3. Chocolate solid and melt.

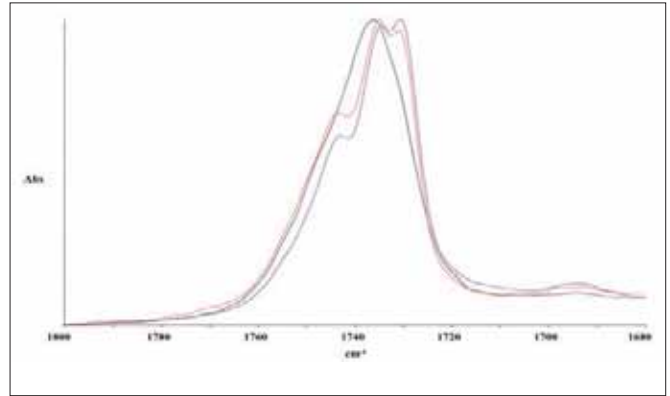


Figure 4. C=O region for chocolate with different thermal histories.

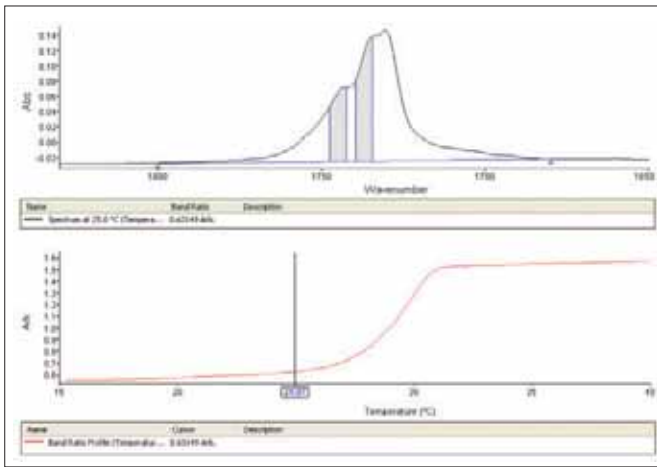


Figure 5a. TimeBase spectral display and band ratio profile for cocoa butter.

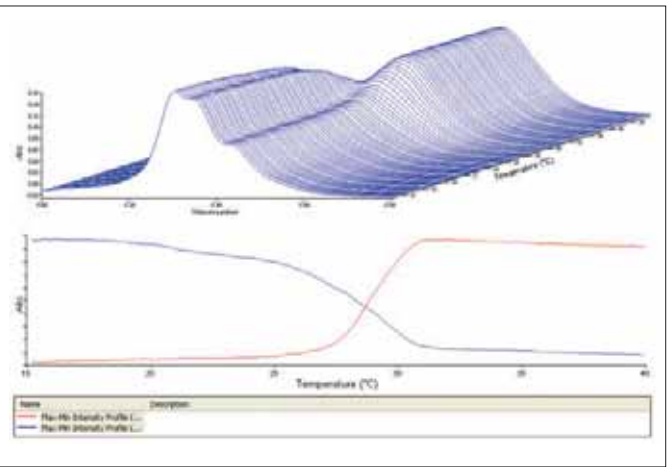


Figure 5b. TimeBase stacked plot and specific band intensity profiles for cocoa butter.

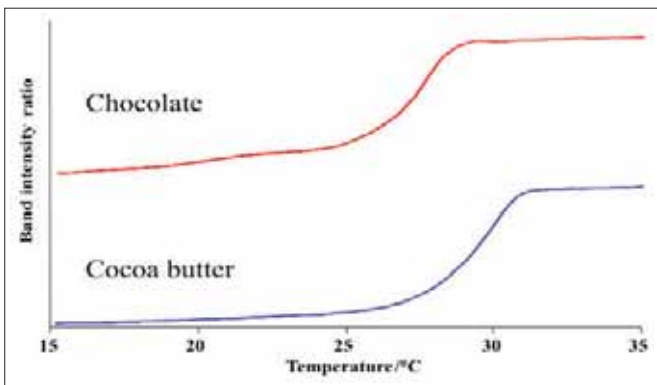


Figure 6. Band intensity ratios for chocolate and cocoa butter.

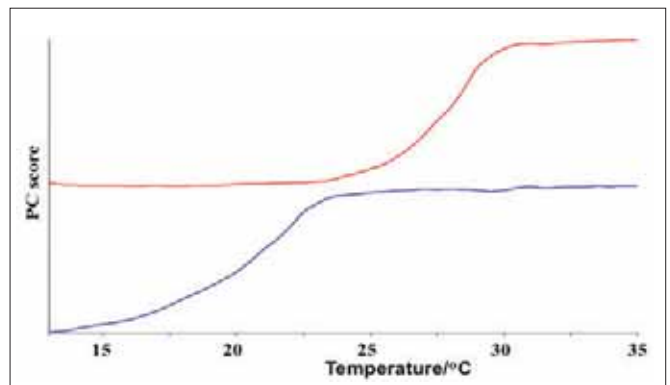


Figure 7. PCA scores for chocolate showing successive transitions.

## Summary

These data show how variable temperature IR measurements can be used to monitor complex phase transitions. The transitions in chocolate are more complex than that seen in cocoa butter. Because the transitions have different spectral signatures they can be separated by choosing to look at different band intensity ratios, or more systematically by using PCA. The spectra at 20 °C show how the thermal history affects the spectra observed at ambient temperatures. Any systematic study to identify the polymorphic changes would require materials with well characterized thermal histories, for example by using Differential Scanning Calorimetry.<sup>1</sup>

As the temperature is raised there is an observable reduction in the intensity of bands due to sucrose compared to those from the cocoa butter. This implies that the cocoa butter concentration at the crystal surface increases, displacing sucrose.

## References

1. 'Characterization of Chocolate Using Power Compensated DSC' PerkinElmer Thermal Analysis Application Note. PETech-43.
2. Lindt & Sprüngli AG, Kulrich, Switzerland, courtesy of W. Böttcher.

## UHPLC

## Author

Padmaja Prabhu

PerkinElmer, Inc.  
Shelton, CT 06484 USA

## Analysis of the Mycotoxin Patulin in Apple Juice Using the Flexar FX-15 UHPLC-UV

### Introduction

Patulin is produced by various molds, which primarily infect the moldy part of apples. Removing the moldy and damaged parts of the fruit may not eliminate all the patulin because some of it may migrate into sound parts of the flesh.

Also, patulin can be produced within the fruit, even though it may not be visibly moldy. If moldy apples are used to produce apple juice, the patulin goes into the juice. It is not destroyed by heat treatments such as the pasteurization process. Patulin is a natural human toxin and therefore can have genetic affects within cells, including a developing fetus, the immune system and the nervous system. The recommended advisory level is 50 µg of patulin/kg in apple juice [50 parts per billion (ppb)].<sup>1</sup> Hydroxymethylfurfural (HMF), also 5-(Hydroxymethyl)furfural, is an organic compound derived from dehydration of sugars. HMF has been identified in a wide variety of heat-processed foods including milk, fruit juices, spirits, honey, etc.<sup>2</sup>

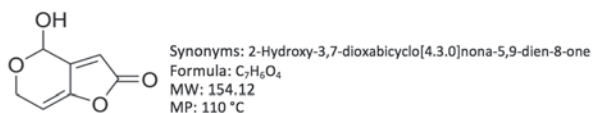


Figure 1. Structure and properties of patulin.

This application note will demonstrate a rapid method for the identification and quantification of patulin in apple juice using high performance liquid chromatography with UV detection. In addition to method optimization and standard analysis, a number of apple juice samples for patulin were analyzed. The samples were randomly collected from the local market in Mumbai.

Patulin is a colorless to white crystalline solid. It is soluble in water, methanol, ethanol, acetone, and ethyl or amyl acetate and less soluble in diethyl ether and benzene.

## Experimental

The PerkinElmer® Flexar™ FX-15, Ultra High Performance Liquid Chromatograph (UHPLC), equipped with a programmable wavelength UV/Vis detector was used for this application. Table 1 presents the detailed operating parameters of the UHPLC and the extraction process of patulin from juice. The instrument interaction, data analysis and reporting was completed with the PerkinElmer Chromera® data system.

**Table 1. Detailed instrument conditions used in the determination of patulin.**

Instrument	Flexar FX-15 High Performance Liquid Chromatograph
Analytical Column	Brownlee™ analytical DB AQ C18 1.9 μm x 100 x 2.1 mm column
Column Temp.	35 °C
Flow Rate	0.5 mL/min
Mobile Phase A	Water pH 4.0 with acetic acid
Mobile Phase B	Water : Acetonitrile (50:50)
Injection volume	25 μL
Wavelength	275 nm
Extraction Procedure	10 mL of apple juice + three extracts with ethyl acetate, combine the three extracts and add 4 gm NaSO <sub>4</sub> . 25 mL of this extract was evaporated to dryness under a stream of nitrogen. The residue was dissolved in 300 μL of mobile phase A and injected in to the chromatographic system.

**Stock Solution of Patulin:** 200 μg/mL of patulin was prepared in ethyl acetate.

**Stock Solution of HMF:** 200 μg/mL of HMF was prepared in ethyl acetate.

**Resolution Standard Solution:** 100 μL each of the stock patulin and HMF were evaporated to dryness in a 10 mL flask, and the residue was dissolved in mobile phase A. This gave a 2 μg/mL mixture of patulin and HMF.

**Preparation of Spike Solution:** 250 μL of stock solution of patulin was evaporated to dryness under a stream of nitrogen and the residue was dissolved in mobile phase A. This gave a 5 μg/mL solution of patulin.

**Calibration Curve:** Varying volumes of 5 μg/mL patulin were spiked into 10 mL of juice samples to produce the following calibration curve (Table 2).

**Table 2. Scheme used for the creation of a six level calibration.**

Cal Level	Volume of Juice (mL)	Std Sol Added (μL)	Final Conc. Patulin (ppb)
1	10	20	10
2	10	40	20
3	10	80	40
4	10	100	50
5	10	160	80
6	10	200	100

**Calibration:** The UV detector was calibrated across the range of 10 to 100 ng/mL; each calibration point was run in duplicate to demonstrate the precision of the system. The average coefficient of determination for a line of linear regression was 0.998 for patulin. The calibration curve for patulin is depicted in Figure 3. The precision of the system across the calibration range is excellent. The chromatograms from the analysis of standard material are shown in Figure 4.

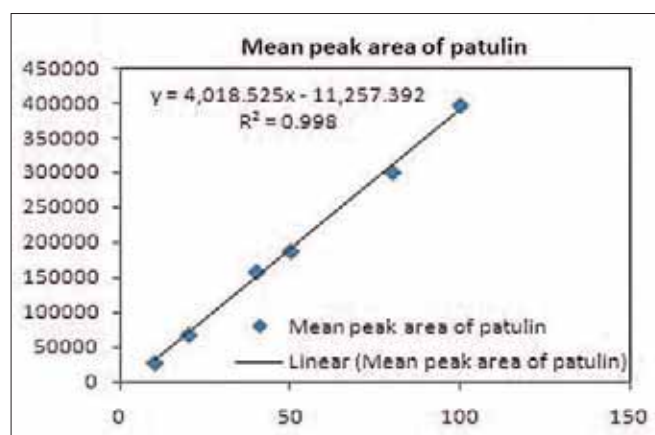


Figure 3. Calibration curve for patulin.

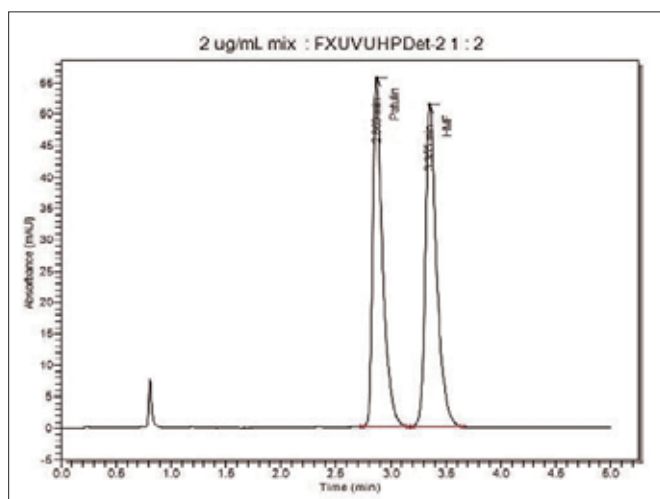


Figure 4. Example chromatogram for patulin.

The precision of the method was measured at both 5.0 and 10 ppb. The loss of precision below 10 ppb indicates the detection limit of this method to be approximately 5 ppb (Table 3).

**Table 3. RSD values for detection limit and quantification level.**

Sr. No.	Conc. of Patulin in ppb	Area of Patulin	Conc. of Patulin in ppb	Area of Patulin
1	5	14894.7	10	41189.2
2	5	18836.3	10	44147.4
3	5	25627.5	10	45305.8
4	5	33795.2	10	44107.4
5	5	30614	10	39631.3
6	5	30640.4	10	43282.5
Mean		25734.6		42943.9
S.D.		7455.87		2123.57
%RSD		<b>28.97</b>		<b>4.94</b>

#### Summary of Method Validation Experiment

**Linearity:** 10.0 ppb to 100 ppb of patulin

**RSD for replicate analysis:** for 10.0 ppb 4.94%

**Detection level:** 5.0 ppb

**Quantification level:** 10.0 ppb

**Recovery study:** at three levels for all the samples 80.52-109.48%

**Sample Preparation:** Samples were collected from the local Mumbai market. Samples included apple juice and apple squash. All the samples were refrigerated until analysis. Ten ml of juice sample was transferred into a 50 mL tube. The juice was extracted three times with 10 mL ethyl acetate. The three extracts were combined and 4 g of sodium sulphate was added to it, to remove moisture. 25 mL of the ethyl acetate layer was then evaporated (to dryness) under a stream of nitrogen. The residue was then reconstituted in 300  $\mu$ L of mobile phase A, filtered through 0.2  $\mu$ m nylon 66 syringe filter from Millipore® and 25  $\mu$ L was injected in to the chromatographic system.

#### Method Validation

The recovery of the method was tested with the juice sample spiked at 3 different levels: 35, 50, 75  $\mu$ g/L. The measured amount was 32.53, 47.49, 63.15  $\mu$ g/L demonstrating that the technique is quantitative in its extraction of patulin from an aqueous matrix.

#### Results

Three samples of apple juice and one squash sample were analyzed using the method developed here.

Sample No.	Sample Details	Amount of Patulin Found in ppb
Sample 1	Juice T	N.D.
Sample 2	Juice S	N.D.
Sample 3	Juice R	N.D.
Sample 4	Apple squash	N.D.

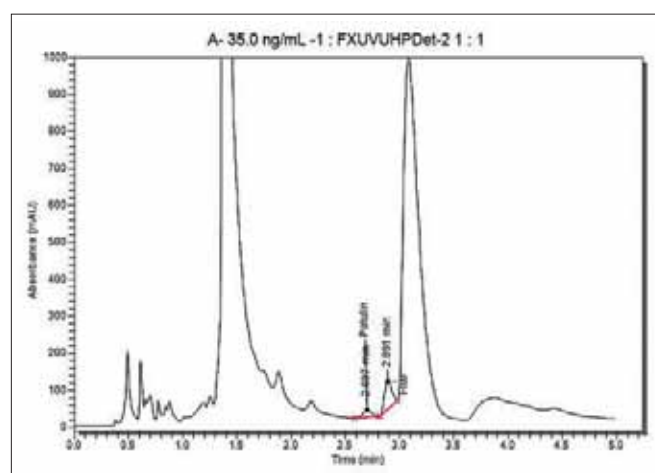


Figure 5. Chromatogram of patulin peak in sample.

## Discussion and Conclusion

This application presents a method for the determination of patulin in apple juice. The method uses a Brownlee analytical DB AQ C18 1.9  $\mu\text{m}$  x 100 x 2.1 mm column with a mobile phase of water of pH 4.0 with acetic acid. The flow rate is 0.5 mL/min. HMF elutes very close to patulin, therefore, it was necessary to demonstrate the separation between patulin and HMF. Ethyl acetate was used for the extraction of patulin and the extracts were treated with sodium sulphate to remove moisture. This was important because patulin may be destroyed when wet ethyl acetate is evaporated to dryness.<sup>3</sup> Also, a lower temperature of 40 °C was used for evaporation of the ethyl acetate layer, since patulin is not stable at high temperatures in ethyl acetate.

Alternately, a Brownlee validated AQ C18 100 x 2.1 mm x 3.0  $\mu\text{m}$  can be used at a flow rate of 0.7 mL per min to achieve the same resolution between patulin and HMF.

The samples collected from the market were analyzed by the above method and the level of patulin determined. All the samples contained less than 5  $\mu\text{g/L}$  of juice. The method was validated at several levels on juice matrix and the recovery values were between 80.52-109.48%.

## References

1. Guidance on the control of patulin in directly pressed apple juice, <http://www.newark-sherwooddc.gov.uk/ppimageupload>.
2. Wikipedia.
3. AOAC Official Method 995.10, Patulin in Apple Juice, Liquid Chromatographic Method.
4. Journal of AOAC International, Vol. 90, No. 3, 879-883.

## Atomic Absorption

**Author:**

Lee Davidowski, Ph.D.

PerkinElmer, Inc.  
Shelton, CT 06484 USA

# Determination of Aluminum in Serum in Customer-Validated Applications using THGA and Longitudinal Zeeman Atomic Absorption

**Introduction**

Determinations of aluminum (Al) in serum are performed routinely by laboratories through customer-validated applications. Graphite furnace atomic absorption spectroscopy (GFAAS) is one of only a few routine techniques with a dynamic range sensitive enough to be used clinically in customer-validated applications to measure Al in serum. There are a few specific analytical challenges that an analyst must consider in

the determination of Al in serum by GFAAS. The serum matrix contains an organic carbohydrate fraction as well as a considerable level of inorganic salts, all of which can interfere with an accurate GFAAS measurement. Some means of reducing these interferences must be considered. Aluminum is also a commonly occurring element such that pronounced external contamination of the sample can occur during the sample-handling phases of the analytical method. Minimal analyst interaction with the sample prior to analysis is needed in order to reduce the chance and degree of contamination.

This work will describe a simple, direct procedure for the analysis of aluminum in serum with aqueous calibration, using small sample volumes, STPF concepts and Zeeman background correction, over a wide range of serum concentrations and with minimal sample interaction.

## Experimental

### Reagents

The sample diluent/modifier solution consisted of 0.1% nitric acid (v/v), 0.01% Triton X-100 and 0.2%  $Mg(NO_3)_2$ . It was prepared from ASTM® Type I deionized water (18M $\Omega$ ), 1%  $Mg(NO_3)_2$  modifier solution (Part No. B0190634), and Triton® X-100 nonionic detergent (Part No. N9300260). Instrument calibration standards were prepared from an aluminum stock standard (PerkinElmer Pure, Single-element Al standard, Part No. N9300184). Bi-Level Trace Element Control freeze-dried Serum samples were from UTAK® Laboratories, Inc. (Valencia, CA).

### Instrumental Conditions

All measurements were made using a PerkinElmer® PinAAcle™ 900T flame and longitudinal Zeeman furnace atomic absorption spectrometer (Figure 1) which includes a transversely heated graphite atomizer and longitudinal Zeeman-effect background correction. Standard tubes (Part No. B0504033) were used for all analyses. The spectrometer was equipped with an AS 900 autosampler and 2.5 mL polypropylene autosampler cups (Part No. B3001566). The system was controlled by WinLab32™ for AA software running under Microsoft® Windows® 7 operating system.



Figure 1. PinAAcle 900T atomic absorption spectrometer with AS 900 furnace autosampler.

Particularly for aluminum analyses, the graphite tube design plays a vital role in the overall sensitivity and stability of the analysis. Aluminum is volatilized as a stable oxide which only partially dissociates when atomization is from the tube wall due to the low gas-phase temperatures at the time of volatilization. With platform atomization, however, volatilization is delayed until the gas phase has reached a higher,

steady-state temperature, thereby increasing atomization efficiency three-fold. Additionally, the patented THGA tube design provides a uniform temperature distribution over its entire length, ensuring not only maximum sensitivity, but also freedom from interferences by eliminating gas-phase analyte recombinations that normally occur at the cold ends of non-THGA tubes.

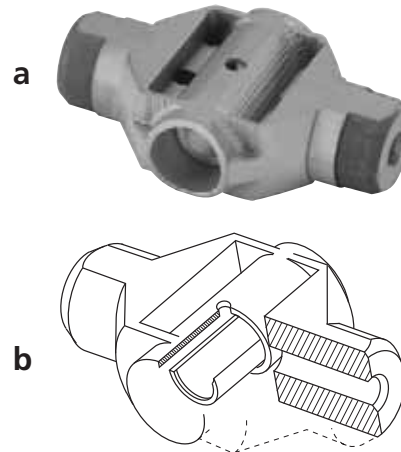


Figure 2. a) Standard THGA tube with integrated L'vov platform. b) Cutaway view of THGA tube.

The THGA tube, with its unique integrated platform (Figure 2), is machined from a single block of graphite and is pyrolytically coated to ensure maximum performance and lifetime.

### Sample Analysis

The commercial freeze-dried bi-level serum control materials were reconstituted with laboratory DI water as per the manufacturer's directions. Thereafter, the control samples are treated the same as any serum patient sample. One mL of serum was transferred with a mechanical pipette into a pre-rinsed autosampler cup. One mL of the diluent/modifier solution was then added (yielding a 1+1 diluted serum). The sample was mixed by repeated pipetting until the diluted sample appeared totally mixed. A "diluent blank" was prepared by mixing one mL DI water with one mL of the diluent/modifier. The aluminum calibration standards were diluted from a 100  $\mu\text{g/L}$  Al standard which was prepared in 50% diluent/modifier solution. The instrument then constructed a multi-point calibration curve by diluting the "stock" 100  $\mu\text{g/L}$  standard with appropriate volumes of the diluent blank solution to levels of 100, 50 and 25  $\mu\text{g/L}$  (Figure 3).

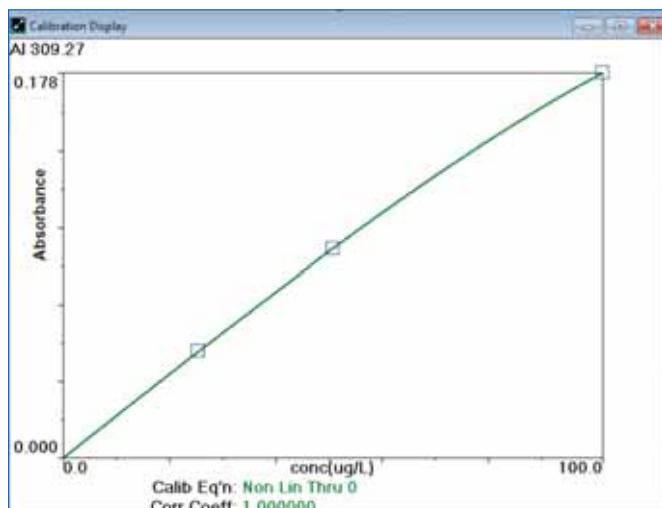


Figure 3. Calibration curve for aluminum in serum using peak area (Abs-sec).

The instrumental parameters and furnace heating program are given in Tables 1 and 2. Due to the slightly more challenging drying characteristics of the of the 1+1 serum sample matrix, 3 drying steps were used. The Triton® X-100 aids in releasing the serum cleanly and reproducibly from the plastic pipette tip. The PinAAcle 900T's TubeView™ furnace camera (Figure 4) is a great benefit in checking the position of the pipette tip and in optimizing the drying times and temperatures for the serum matrix.

<b>Table 1. Instrumental parameters of PinAAcle 900T for measurement of aluminum in serum.</b>	
Component/Parameter	Type/Value/Mode
Wavelength (nm)	309.27
Source Lamp (current)	Al HCL (25 mA) (Part No. N3050103)
Slit Width (nm)	0.7
Background Correction	Longitudinal AC Zeeman-effect
Measurement Mode	Peak Area, 3 Replicates
Calibration Algorithm	Non-Linear Through Zero
Integration Time (s)	5.0
Sample Volume (µL)	12
Calibration Stds. (µg/L)	25, 50, 100
THGA	Standard THGA Tube

<b>Table 2. Temperature program for the measurement of aluminum in serum using THGA.</b>					
Step		Temp. (°C)	Ramp Time (sec)	Hold Time (sec)	Argon Gas (mL/min)
1	Drying	120	1	10	250
2	Drying	140	5	10	250
3	Drying	200	5	5	250
4	Pyrolysis	1200	5	15	250
5	Atomization	2300	0	5	0
6	Clean-out	2450	1	3	250

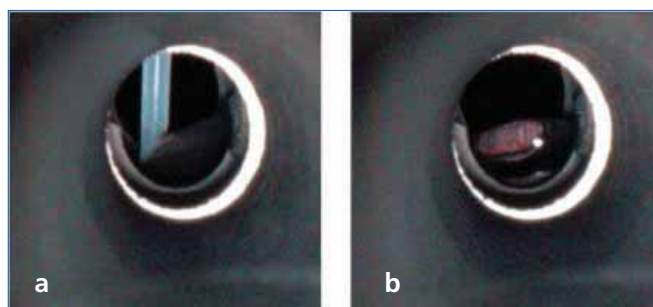


Figure 4. TubeView furnace camera captures of AS 900 pipette in graphite tube during sample deposition.

## Results

The sensitivity of a method can be defined as the characteristic mass ( $M_0$ ), the mass of the element injected into the furnace that yields a background-corrected signal of 0.0044 Abs.sec. A characteristic mass of 29 pg was found for Al, which is in very close agreement with the manufacturer's recommended  $M_0$  value of 31 pg. Due to serum matrix components, a slight difference in the appearance time of the atomic signal and the peak shape was found as compared to the aqueous standard (Figure 5). This, however, is not a problem when using STPF conditions. Peak area signal processing is used here so that the entire Al signal is measured and quantified, regardless of appearance time and peak shape. This method of quantification was used for all analyses and samples.

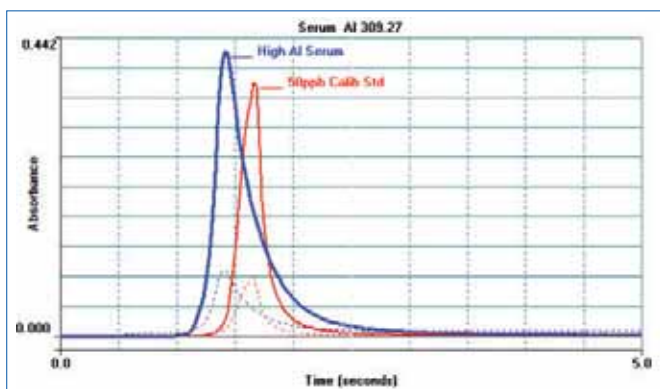


Figure 5. Solid lines represent Al atomic absorption profile signals for 50 µg/L Calibration Standard (Red) and High Range Serum Control (Blue). Dashed lines represent the background absorption profiles.

The results of the serum analyses are shown in Table 3. The concentration values are corrected for the in-lab dilution. The serum control samples show very good agreement with the expected values. Using the STPF principles of platform atomization and proper matrix modification, it is shown that a simple aqueous calibration scheme can be used for detection of Al in serum samples. The standard deviation and relative standard deviation (%RSD) values (Table 3) show relatively good reproducibility for these 1+1 serum solutions. Based on the standard deviations of the normal level serum and/or the diluent blank determinations, this method yields a method detection limit of less than 1 µg/L (<0.04 µmol/L) of Al in serum.

**Table 3. Corrected results for the analyses of aluminum in serum (µg/L).**

Sample ID	Verified Value	Expected Range	Found Mean	Std Dev	%RSD
Normal Range	12	7.2 – 16.8	11.1	0.4	3.6%
High Range	176	141 - 211	198	3	1.6%
Diluent Blank			0.52	0.03	

## Conclusion

Using the PinAAcle 900T atomic absorption spectrometer, aqueous calibration standards, and a simple 1+1 dilution, this method has been successfully applied to the determination of aluminum in serum. Bi-level serum controls showed the method to be simple, reliable, accurate and precise. The reduced sample handling keeps the risk of contamination and sample preparation time to a minimum. This application procedure has a wide dynamic range with a method detection limit well below the normal range of aluminum in serum. It also covers the higher aluminum concentrations found in medically exposed samples. By employing the latest analytical concepts of the stabilized temperature platform (STPF) technique and the instrumental advances of transversely heated graphite atomizer (THGA) tubes, chemical interferences are overcome allowing for faster, simpler direct calibration. The PinAAcle 900T atomic absorption spectrometer is suitable for clinical use in customer-validated applications for the measurement of aluminum in serum.

## Atomic Absorption

**Author:**

Cynthia Bosnak

PerkinElmer, Inc.  
Shelton, CT 06484 USA

## Using THGA and Zeeman Background Correction for Blood-Lead Determination in Customer-Validated Applications

### Introduction

A reliable clinical-use instrument that facilitates the accurate determination of blood-lead levels in customer-validated applications is in the interest of occupational safety and public health. The CDC (Centers for Disease Control) currently requires action for any blood-lead level concentrations above the current 10 µg/dL guideline.<sup>1</sup>

However, there is no safe threshold

for lead in blood and it is important that any customer-validated application incorporate a clinical instrument that provides accurate and precise measurements.

Validated applications determining whole blood levels are generally performed using graphite furnace atomic absorption spectroscopy (GFAAS). GFAAS is cost effective, allows for detection limits well under the blood-lead level action guideline, and requires less operator training than more advanced elemental techniques.<sup>2</sup> In this study, we will demonstrate the applicability of the PerkinElmer® PinAAcle™ 900T atomic absorption spectrometer (Figure 1) using the stabilized temperature platform furnace (STPF) and transversely-heated graphite atomizer (THGA), for use in customer-validated applications to determine lead amounts in blood samples. Aqueous calibration standards were used instead of matrix-matched blood standards or the method of additions for calibration. This simplifies and minimizes analysis time.

## Experimental

### Preparation of Reagents

All reagents, standards and samples were prepared with ASTM® Type I deionized water (18 MΩ • cm). Concentrated nitric acid (69-70%), HNO<sub>3</sub>, was trace metal grade (TMG) or better.<sup>3</sup>

- **10% Triton® X-100 Stock Solution:** Weigh 10 grams of Triton® X-100 wetting agent (Part No. N9300260) directly into a 125 mL LDPE bottle. Add deionized water up to 100 grams. Shake well to mix thoroughly.
- **Autosampler Rinse Bottle Solution:** Almost fill the 2 L autosampler rinse bottle with deionized water. Add 4 mL of concentrated nitric acid, and 100 µL of 10% Triton® X-100 solution. Shake well.
- **Diluent/Matrix Modifier Solution:** Into a 60 mL LDPE bottle, pipette 1 mL of 10% Ammonium Dihydrogen Phosphate, NH<sub>4</sub>H<sub>2</sub>PO<sub>4</sub>, matrix modifier (Part No. N9303445) and 2.5 mL of the 10% Triton® X-100 Stock Solution, and 0.1 mL of concentrated nitric acid. Dilute to 50 mL with deionized water.
- **1% HNO<sub>3</sub> solution:** Add approximately 500 mL of deionized water to a 1 L plastic volumetric flask. Pipette 10 mL of concentrated nitric acid and dilute to volume with deionized water.
- **Intermediate Standard Solution (10 mg/L):** Pipette 1 mL of 1000 mg/L Lead stock standard (PerkinElmer Pure, Part No. N9300175) into a 125 mL LDPE bottle and bring to 100 g with 1% HNO<sub>3</sub>. Prepare monthly.

### Standard and Sample Preparation

Dilute the 10 mg/L intermediate stock standard to 100, 200, 400, and 600 µg/L secondary standards by adding 1, 2, 4, and 6 mL, respectively, of the 10 mg/L intermediate stock and bringing up to volume in clean 100 mL plastic flasks with 1% HNO<sub>3</sub>.

To make the calibration standards: Into clean 1.2 mL autosampler cups (Part No. B0510397), pipette 100 µL of each secondary solution into 900 µL of diluent/modifier solution. Flush the pipetter up and down 5-10 times to completely mix the solution in the autosampler cup. Repeat the procedure using the 1% HNO<sub>3</sub> solution for the blank.

NIST® Trace Elements in Caprine Blood (SRM 955c) and LyphoChek Whole Blood Metals Controls Levels 1, 2, and 3 (BioRad, Hercules, CA) were used as samples. Samples were diluted directly into the 1.2 mL autosampler cups by pipetting 100 µL of each blood sample into 900 µL of the diluent/modifier solution and mixing as above.

## Instrumentation

A PinAAcle 900T flame and longitudinal Zeeman furnace atomic absorption spectrometer was used for all measurements. A PerkinElmer Lumina™ single-element Pb hollow cathode lamp (Part No. N3050157) was used as the light source and argon was the normal gas type. The PinAAcle 900T instrument settings are listed in Table 1 and the furnace program used for all samples is listed in Table 2.



Figure 1. PinAAcle 900T atomic absorption spectrometer with AS 900 furnace autosampler.

**Table 1. Instrument Settings for the PinAAcle 900T.**

Parameter	Value
Wavelength:	283.3 nm
Slit:	0.7 nm
Lamp Current:	10 mA
Integration Time:	4 s
Calibration Type:	Linear through zero
Replicates:	2
Standard Units:	µg/dL
Sample Units:	µg/dL
Sample Volume:	12 µL
BOC:	2 s

**Table 2. Furnace program for measuring Pb in blood samples using a PinAAcle 900T with THGA tubes.**

Step	Temp. (°C)	Ramp (sec)	Hold (sec)	Internal Flow	Read Step	Gas Type
1	120	5	10	250		Normal
2	140	5	10	250		Normal
3	200	10	10	250		Normal
4	700	10	20	250		Normal
5	1500	0	4	0	X	Normal
6	2450	1	3	250		Normal

\*Injection Temperature: 110 °C

Standard pyrolytically-coated THGA tubes (Part No. B0504033) with integrated platforms were used for all analyses. The unique patented design of the THGA tubes provides consistent heating and high atomization efficiency for all elements including refractory elements. The tube and integrated platform are machined from a single block of PerkinElmer exclusive, high-density graphite. The transverse heating of the tube ensures a uniform temperature distribution along the length of the tube, thereby significantly reducing condensation of the matrix components and memory effects. The longitudinal Zeeman-effect background correction provides accurate correction without the loss of light associated with transverse Zeeman systems.

The TubeView™ furnace camera on the PinAAcle 900T was used to adjust the pipette tip to the most appropriate depth (Figure 2a) and to watch for matrix buildup on the platform should it occur. The camera was also used during method development to verify the drying steps and ensure that no sample boiling or splattering occurred (Figure 2b).

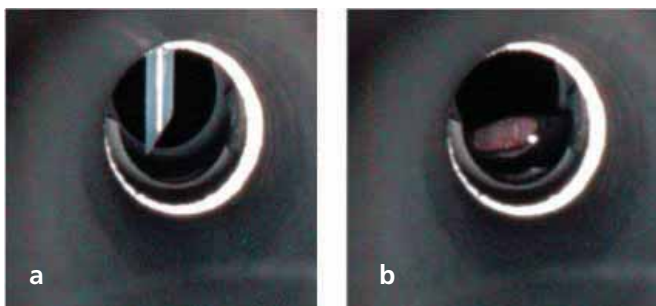


Figure 2. a) AS 900 autosampler alignment as seen using the TubeView furnace camera; b) blank sample inside the THGA during method development.

## Results and Discussion

Aqueous calibration standards are more convenient to use than multiple standard additions steps for Pb in blood analyses. It provides for less operator error, lower cost, and shorter analysis times than with standard additions or matrix matched standards.<sup>4</sup> An overlay of the peak plots for an aqueous Pb standard (red) and a blood reference material (blue) taken on the PinAAcle 900T are shown in Figure 3. As expected, in the blood matrix, Pb volatilization is delayed relative to the Pb in the standard. However, with the STPF conditions used, all Pb atoms are volatilized into a steady-state temperature environment, regardless of appearance time. As a result, each Pb atom contributes equally to the atomic absorption process permitting the use of simple aqueous standard calibration with resulting accuracy and precision.

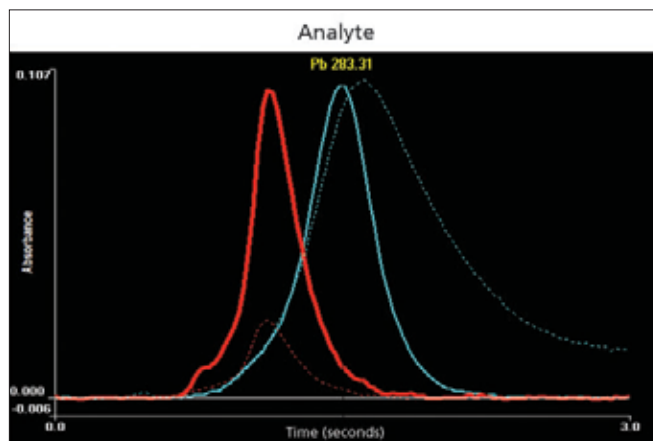
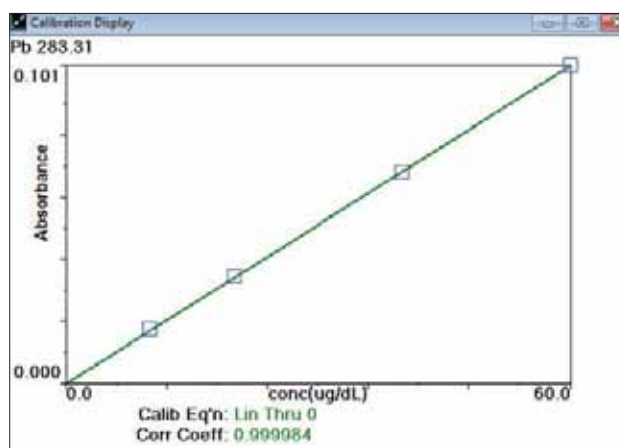
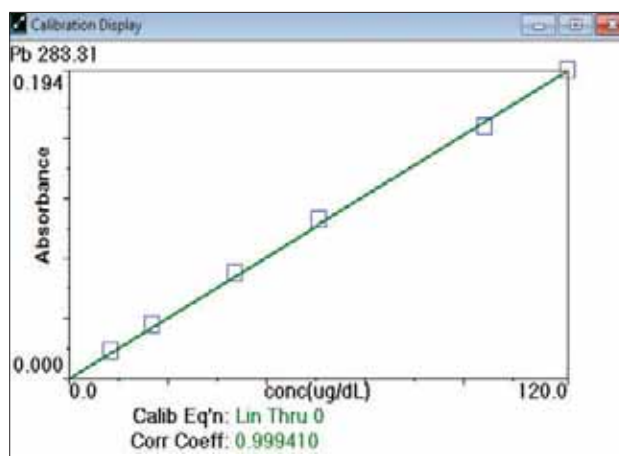


Figure 3. Overlay of an aqueous standard (red lines) and a blood reference material (blue lines). Solid lines are the analytical signal after background correction (AA-BG); dotted lines are the background signal (BG).



a



b

Figure 4. a) Linear calibration curve for Pb samples up to 60 µg/dL. b) Linear calibration curve for Pb samples up to 120 µg/dL.

Although for this analysis, the instrument was calibrated up to 60 µg/dL (Figure 4a), it can be shown that the instrument is linear up to 120 µg/dL or higher (Figure 4b). This provides a means of minimizing the number of sample dilutions that are required for high-level samples. Multiple measurements of the blood diluent solution produced an estimated detection limit of 0.23 µg/dL (3SD).

The NIST® standard reference material 955c, Toxic Metals in Caprine Blood, showed recoveries ranging from 98-102% for all four levels (Table 3). The tri-level BioRad LyphoChek Control samples showed recoveries from 100-106% (Table 4). All experimental values easily fell into the reference value range.

**Table 3. Results for NIST® SRM 955c using aqueous calibration standards and GFAAS.**

Sample	Reference Value (µg/dL)	Experimental Value (µg/dL)	Recovery (%)
Level 1	0.424 ±0.011	0.431	102
Level 2	13.950 ±0.080	13.8	99
Level 3	27.76 ±0.16	27.6	100
Level 4	45.53 ±0.27	44.8	98

**Table 4. Results for tri-level BioRad LyphoChek Control samples.**

Sample	Reference Value*		Experimental Value (µg/dL)	Recovery (%)
	Value* (µg/dL)	Range (µg/dL)		
Level 1	9.58	7.67-11.5	9.83	103
Level 2	27.7	22.2-33.3	29.4	106
Level 3	54.0	43.2-64.8	54.0	100

\* BioRad reference values represent an average from laboratories using ICP-MS.

The AS 900 furnace autosampler was used to ensure accurate delivery of the sample. The AS 900 autosampler probe did not require any cleaning or maintenance between analytical runs to prevent carryover from high-level samples. It can also provide automated dilution of samples outside of the calibration range, if necessary.

## Conclusions

An example of how our instrument can be used in a customer's clinically validated application for lead determination was presented here. The speed and accuracy of a customer-validated application is made possible by using the STPF concept, THGA system and detection with the PinAAcle 900T atomic absorption spectrometer. The linear dynamic range allows measurement throughout a large range of sample concentrations from well below the critical threshold of 10 µL/dL to much higher concentrations that may be needed for both clinical and research applications. The PinAAcle 900T atomic absorption spectrometer is suitable for clinical use in customer-validated applications for the measurement of lead in blood.

## References

1. "Graphite Furnace Atomic Absorption Spectroscopic Measurements of Blood Lead in Matrix-Matched Standards", Bannon, D.I., Murashchik, C., Zapf, C.R., Farfel, M.R., Chisollm, J.J. Jr. Clinical Chemistry • Automation and Analytical Techniques, Vol. 40, No. 9, pp. 1730-1734, 1994.
2. "An Assessment of Contemporary Atomic Spectroscopic Techniques for the Determination of Lead in Blood and Urine Matrices", Patrick J. Parsons, Ciaran Geraghty, Mary Frances Verostek, Spectrochimica Acta Part B, Vol. 56, pp. 1593-1604, 2001.
3. "Blood Lead Determination by Electro-thermal Atomization Atomic Absorption Spectrometry with PerkinElmer 4100ZL AAS", New York State Department of Health, May 19, 1992.
4. "A Rapid Zeeman Graphite Furnace Atomic Absorption Spectrometric Method for the Determination of Lead in Blood", Patrick J. Parsons and Walter Slavin, Spectrochimica Acta, Vol. 48B, No. 6/7, pp. 925-939, 1993.

## FT-IR Spectroscopy

**Authors****J. Neal-Kababick****Flora Research Laboratories  
Grants Pass, OR USA****P. Courtney, J. Sellors and C. Lynch****PerkinElmer, Inc.  
Shelton, CT USA**

## Rapid Authentication of Larch Fiber Dietary Supplement Ingredient by FT-IR Using Diamond Single Bounce uATR Sampling Device

**Introduction**

Larch fiber is a complex botanical material rich in arabinogalactin containing polymers that has shown promise as an immune-stimulating and pre-biotic dietary supplement. However, due to the highly complex nature of the material, it does not lend itself to easy identification using microscopy or thin layer chromatography; two common methods used to authenticate dietary supplements. In order to comply with the new Dietary Supplement current Good Manufacturing Practices (cGMP's), all dietary ingredients

must be identified using a valid scientific method. A PerkinElmer MIR/NIR spectrometer equipped with a single-bounce diamond uATR sampling accessory allows for rapid identification of larch fibers of various grades. Even though there is some variance among samples, the fingerprint region has a consistent profile that is unique and easily recognized. Differentiation between authentic larch fiber and common potential economic adulterants (cellulose and carageenan) is achieved using this method. FT-IR is a very well established methodology for identification of chemical compounds and can be utilized to comply with the 21 CFR Part 111 cGMP's for Dietary Supplements. Using the Enhanced Security software meets the requirements of 21 CFR Part 11 which is also called for in the Dietary Supplement cGMP's.

## Authentication of Dietary Supplement Ingredients

An ideal identity method would be a) fast, b) simple, c) able to differentiate larch fiber from other commonly utilized ingredients and d) robust enough to tolerate slight changes in the finished product as a result of manufacturing differences. As will be shown here, the use of FT-IR (MIR) coupled with the uATR sampling accessory meets these conditions.

Larch fiber polymers can range from 10,000-120,000 Daltons. The typical ratio of galactose to arabinose units is 6:1. An analysis of the sugar ratios can help confirm identity but this is both a time and resource intensive process. Yariv reagents can also be utilized in the analysis of larch fiber arabinogalactins but these are proprietary and costly reagents and, like sugar profiling, requires a high level of technical skill.

The color of larch fiber is white to off-white and it has a powder consistency which can create challenges for visual identification. Various processing methods create variations in the appearance. Further, it can easily be substituted with other products commonly used in manufacturing supplements making economic or unintentional adulteration a concern.

## Experimental

Materials used in this study are the following:

1. Larch Arabinogalactin – (Fluka® brand) Sigma-Aldrich®, St. Louis, MO
2. Gum Arabic (from acacia) – Sigma-Aldrich®, St. Louis, MO
3. Cellulose Powder & Maltodextrin – gifts of Dr. Andrew Halpner
4. Carageenan – Research Organics®, Cleveland, OH
5. Larch Fibers (Lonza & Spectrum) – gifts of Dr. Anthony Smith

The PerkinElmer MIR/NIR spectrometer is capable for both near infrared (NIR) and mid infrared (MIR) operation, used with a single bounce diamond uATR sampling accessory fitted with conical pressure plate and adaptor for 0.5 mm shoe for 1 or 3 bounce plates (Part No. L1202049).



*Figure 1.* Close-up view of pressure arm and uATR crystal with conical shoe and adaptor.

Data acquisition was carried out using the following procedure:

- Place a small amount of sample on the uATR accessory to cover the crystal
- Compress with pressure arm until ~70% transmission is achieved
- Collect spectra from 4000 – 650  $\text{cm}^{-1}$

Sample analysis involved post acquisition use of automated data processing using “Data Tune Up” to correct for the distortion caused by uATR. Data were compared on-screen and interpreted by visual inspection. Maltodextrin and larch arabinogalactin were further analyzed using the data comparison software to demonstrate automated matching.

## Results and Discussion

A comparison of the spectra obtained from the three larch materials used in this study show close agreement in the fingerprint region (Figures 2 and 3). Slight differences from water bands are due to differing levels of moisture.

## Conclusion

While some materials may require library matching or the formation of derivatives, the unique profile of larch fiber readily allows for authentication by FT-IR based on visual inspection. A “Compare” analysis of larch fiber and maltodextrin showed a match quality of 0.56 (2000  $\text{cm}^{-1}$  to 650  $\text{cm}^{-1}$ ) whereas arabinogalactin larch standard match quality was >0.80 demonstrating that comparison against a reference set using automated software analysis is also possible. The mid-IR data differs from near-IR in that a visual inspection of the transmission spectra is often adequate to confirm identity. This is especially true when working with pure chemical compounds. Finally, the ability to compress samples with real-time instrument read back of force gauge pressure helps assure consistent spectra and good reproducibility.

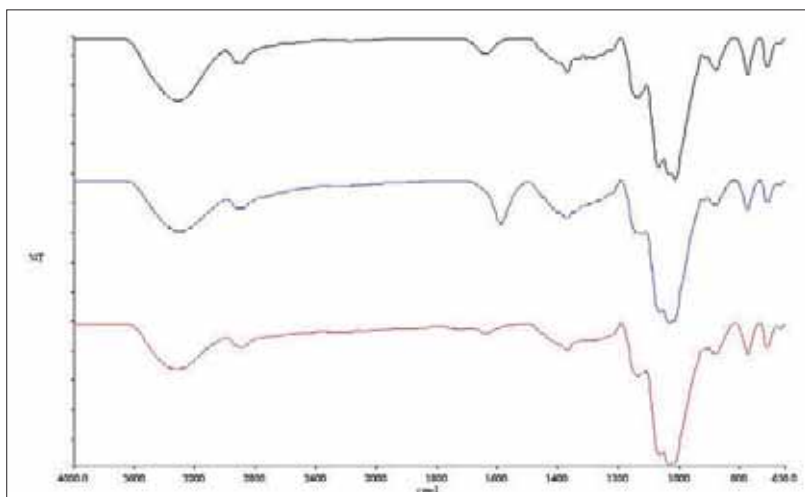


Figure 2. Larch fiber samples stacked full scan for three genuine samples.

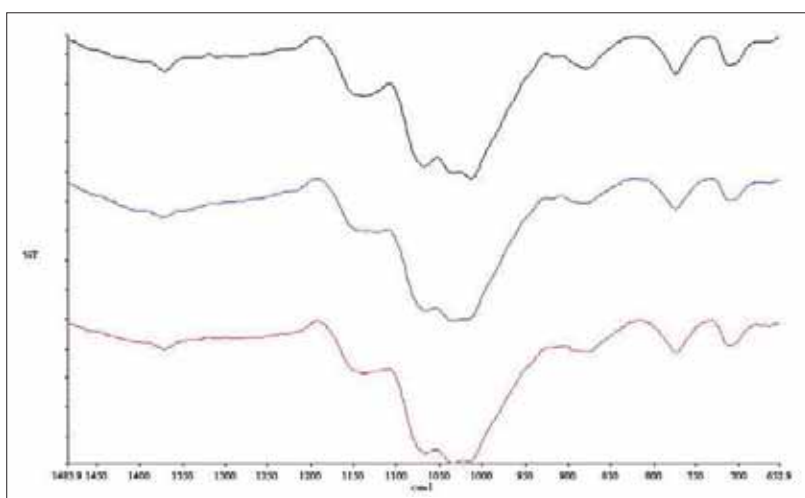


Figure 3. Fingerprint region (1450 – 650  $\text{cm}^{-1}$ ) of larch samples showing consistent profile between three genuine samples of larch fiber.

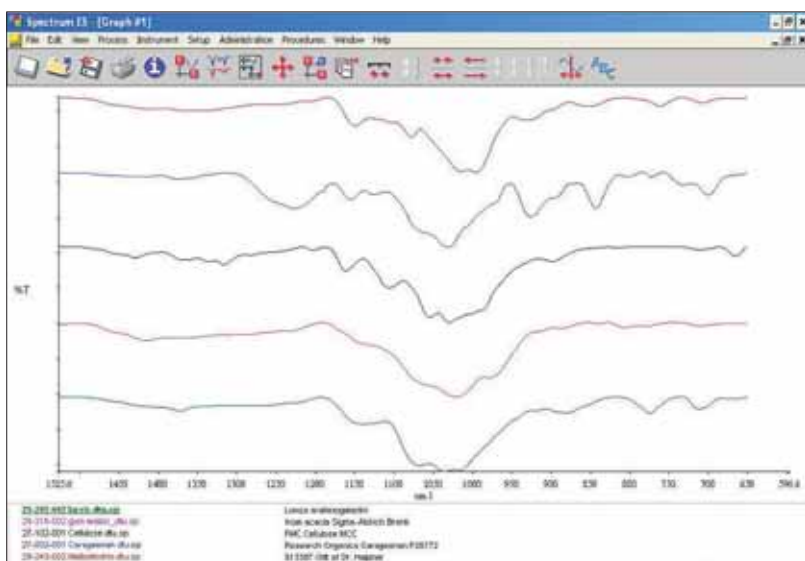


Figure 4. Screen shot of fingerprint region of larch fiber and various potential adulterants (top-red Maltodextrin, middle-upper-blue Carageenan, middle-black Cellulose, middle-lower-pink Acacia Gum Arabic, bottom-green Arabinogalactin).

## References

1. Lonza Fiberaid specification sheet USA3-30009.
2. Alternative Medicine Review Vol 5 #5 2000 pg 463-466
3. 2009-2010 USP Dietary Supplements Compendium.
4. Federal Register – 21 CFR Part 111 (Code of Federal Regulations).
5. Infrared Spectral Interpretation – A Systematic Approach, Brian Smith CRC Publishers 1999.

## Acknowledgement

A special thanks to Dr. Andrew Halpner and Dr. Anthony Smith for their generous gifts of authenticated commercial dietary ingredients.

**PerkinElmer, Inc.**  
940 Winter Street  
Waltham, MA 02451 USA  
P: (800) 762-4000 or  
(+1) 203-925-4602  
[www.perkinelmer.com](http://www.perkinelmer.com)



---

For a complete listing of our global offices, visit [www.perkinelmer.com/ContactUs](http://www.perkinelmer.com/ContactUs)

Copyright ©2010, PerkinElmer, Inc. All rights reserved. PerkinElmer® is a registered trademark of PerkinElmer, Inc. All other trademarks are the property of their respective owners.

009489\_01

## Simultaneous TGA-DSC

## Author

Andrew Salamon

PerkinElmer, Inc.  
Shelton, CT USA

## Pharmaceutical Compounds are Analyzed in Half the Time by Simultaneous TGA-DSC

### Introduction

In an aggressive business climate, PerkinElmer improves pharmaceutical laboratory productivity and increases sample analysis throughput by performing two analytical techniques simultaneously. The STA 6000 Simultaneous Thermal Analyzer

performs both Thermogravimetric Analysis and Differential Scanning Calorimetry together, at the same time.

In the "Early Drug Discovery Phase" of pharmaceutical development when there is a minimum amount of synthesized drug candidate, quick thermal analysis using a small amount of sample is the norm. The sample amount could be less than 3 mg. Because of the rush to identify possible drug candidates, analytical answers must be given within the day. The STA 6000 with its sensitivity of 0.1  $\mu\text{g}$  allows minimum sample material to obtain reproducible results in half the time.

This application note examines three typical drug-discovery-type pharmaceutical materials by Simultaneous Thermal Analysis, TGA-DSC.

- Sample A: free-base, small-molecule crystalline powder
- Sample B: HCl salt of Sample A, monohydrate
- Sample C: Mesylate salt of Sample A, trihydrate

## Results

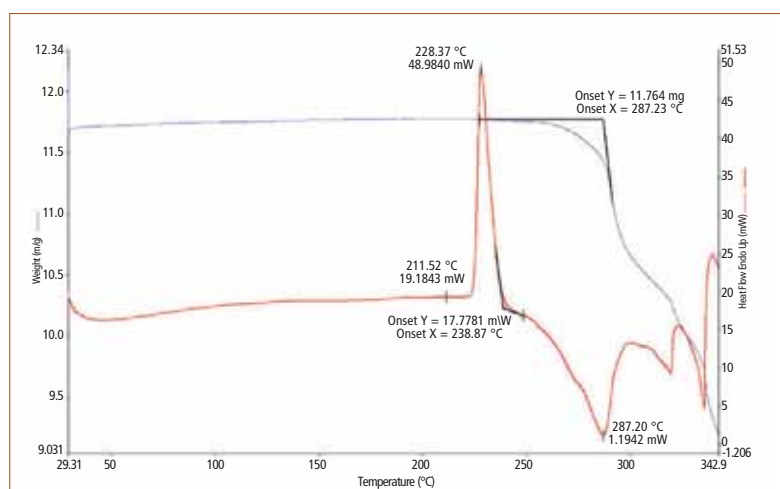


**Figure 1. Sample A:** Sample A characterized by the STA 6000 displays the Red DSC thermal curve and the Blue TGA weight loss curve. Sample A is a free base, small-molecule crystalline powder (11.679 mg). The DSC curve indicates that there is a crystalline melt defined by the peak temperature at 228.37 °C. After the melt transition, the baseline returns to a slightly lower position than the pre-melt baseline. The post-melt baseline changes slope as the sample begins decomposition. The DSC exothermic decomposition peak at 287.2 °C corresponds to the TGA extrapolated onset temperature of 287.2 °C as this sample decomposes.

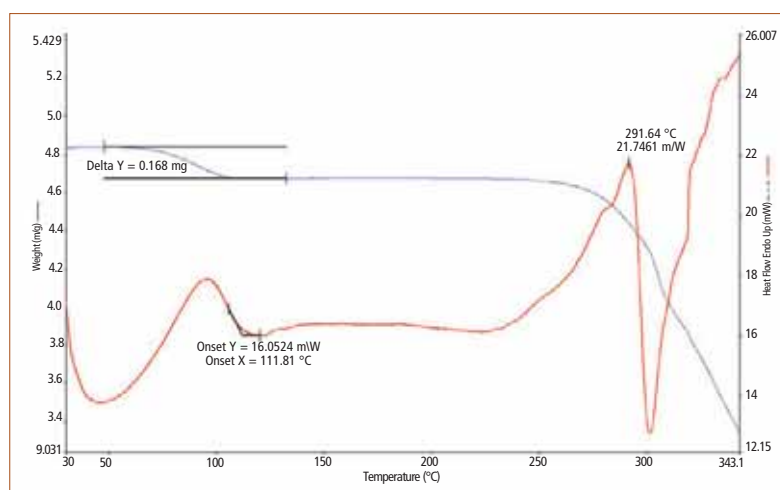


**Figure 2. Sample B:** Sample B (4.89 mg), a HCl salt of Sample A monohydrate, exhibits a weight loss of water upon heating of 0.168 mg. The amount of lost water is measured by a simple delta Y calculation on the TGA curve. It closely matches the calculated value from the stoichiometric 1:1 ratio for a monohydrate. The accompanying DSC thermal curve exhibits a corresponding endothermic reaction that begins just after the start-up transient and concludes at 111.81 °C. The sample continues to heat until it begins an endothermic event at the very beginning of decomposition. This is acknowledged by the onset of the endothermic DSC event and its correlation to the start of the weight loss curve. Then the sample experiences an abrupt decomposition exothermic event beginning at 291.64 °C as displayed by the DSC Peak temperature.

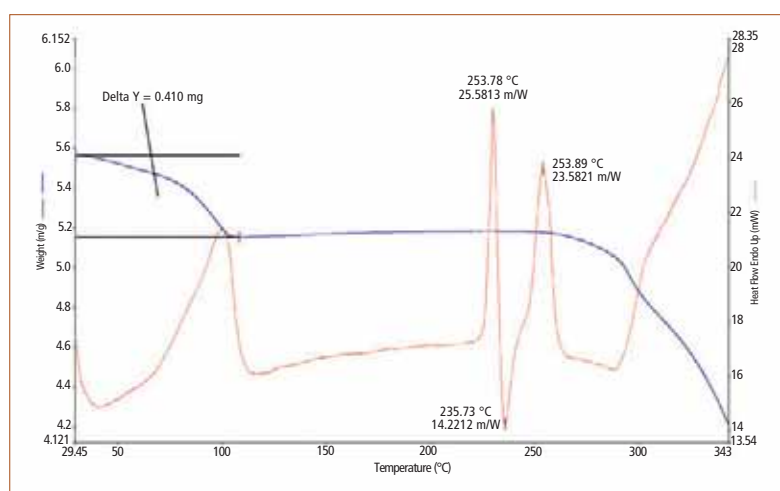


**Figure 3. Sample C:** Sample C (5.562 mg) Mesylate salt of Sample A, exists as a trihydrate. The TGA curve exhibits the surface water weight loss of 0.410 mg, and decomposes above 250 °C. As expected the DSC thermal curve exhibits three peaks. The first DSC endothermic peak is due to the release of all the hydration water from the crystalline lattice. This corresponds to surface water weight loss of 0.410 mg on the TGA curve. The series of endothermic and exothermic events between 215 °C and 270 °C represent a crystal-crystal transformation upon heating, with the initial endothermic peak representing a crystalline melt (an essentially anhydrous crystalline phase since the hydration water was previously removed); the next peak at 236.73 °C, an exothermic event, is a recrystallization of the melted material forming a new crystalline structure, immediately followed by the melt of that crystalline form. The melt-recrystallization-melt series of events are also called a polymorph conversion (phase transition) process. This is a typical characteristic of small-molecules organic crystals.<sup>1</sup> All this occurs just before final decomposition.



## Experimental

The analysis was performed on a PerkinElmer® STA 6000 Simultaneous TGA-DSC, using alumina ceramic pans and a standard furnace. The instrument's furnace was calibrated using a metal reference material's melting temperature. In this case, a single point indium melting event was used to calibrate temperature and heat flow. The instrument's balance was calibrated using a certified weight. The sample purge was dry nitrogen with a flow rate of 30 mL/minute. The large Sample A was run just to show that the STA 6000 can easily run any sample size. The temperature program was from 30 °C to 350 °C, with a scanning of 10 °C/minute.

Sample Weights:

- Sample A: 11.679 mg
- Sample B: 4.829 mg
- Sample C: 5.562 mg

## Conclusion

The STA 6000 provides the productivity that pharmaceutical companies and others are seeking. It combines DSC and TGA thermal techniques to give the user reproducible results in half the time. Designed with routine and research applications in mind, the STA 6000 Simultaneous Thermal Analyzer applies leading edge sensor technology to yield higher accuracy and quality results. The patent pending SaTurnA™ sensor and proven compact furnace ensure better temperature control, more consistent measurements, and the fastest cool-down time. To further productivity, the STA 6000 with its easy-to-load vertical system can be equipped with an autosampler that runs an unprecedented 45 samples unattended.

## Acknowledgement

1. PerkinElmer thanks Dr. Ilie Saracovan, Material Scientist and Consultant, for his comments in regard to the content of this application note.

## FT-NIR Spectroscopy

## Solid Materials Checking Using the Near-IR Reflectance Accessory (NIRA)

### Versatility of Sampling

The NIR Reflectance Accessory (NIRA) for the PerkinElmer Frontier™ System is designed for quick, easy sampling without compromising spectral quality. Sampling is simple as materials are measured directly in containers placed on the rugged sample platform. In the case of tablets, tablet blister packs, and transdermal patches,

samples are placed directly on the sampling window where they are illuminated from below. Samples can also be measured in a range of containers, from conventional vials, plastic bags or bottles, to colored glass bottles. The original containers which the samples are transported to the instrument are more convenient, reproducible, and carry less risk of cross-contamination than using fiber-optic dipping probes.

To illustrate the versatility of NIRA sampling, a few examples and their resultant spectra are shown in this note.

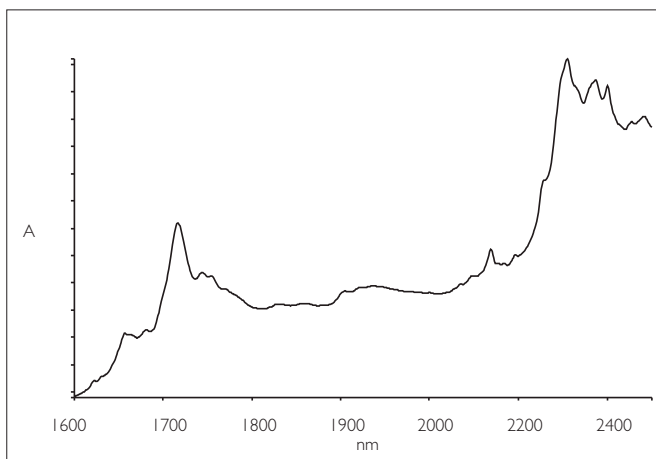


Figure 1. NIR spectrum of aspirin tablet in pack. It is unnecessary to remove a tablet from a blister pack before obtaining the spectrum using the NIRA. Simply place the sample you want, in its blister packing, directly on the sampling window.

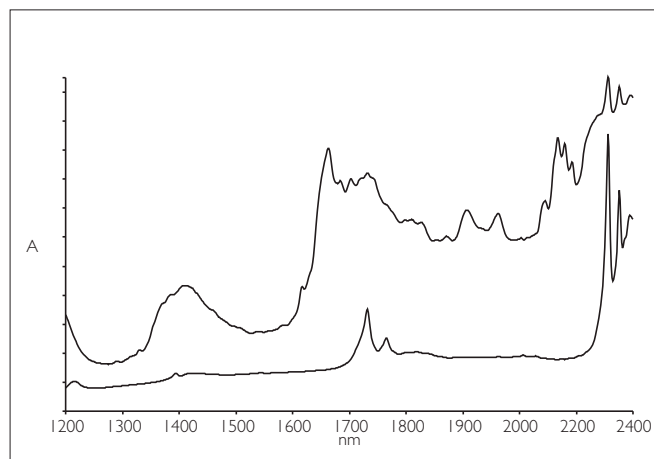


Figure 3. NIR spectra of a polyethylene bag (lower) and polybutylene terephthalate (PBT) in a polyethylene bag (upper). This PBT sample was received in a polyethylene bag, and scanned intact.

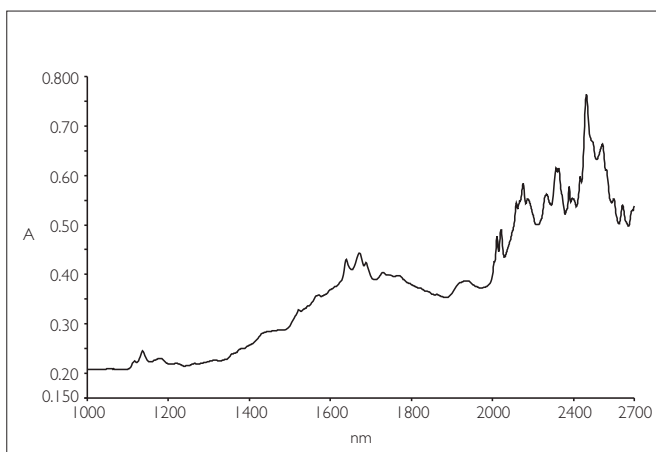


Figure 2. NIR spectrum of paracetamol tablet. The spectrum of a paracetamol tablet was obtained by simply placing the tablet on top of the sampling window.

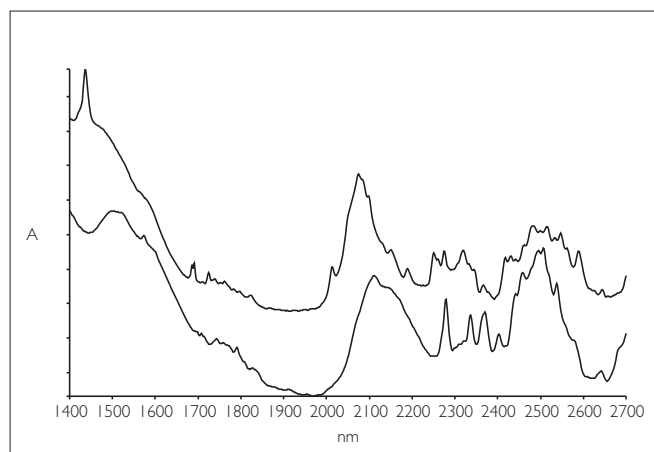


Figure 4. NIR spectra of sucrose (upper) and dextrose (lower) scanned in amber colored glass vials.

### Advantages of the NIRA Accessory

By eliminating the need for any special sample preparation or accessory cleaning, the NIRA ensures more consistent measurement conditions. The large illumination area allows for the analysis of samples with varying (large) particle size and inhomogeneity is improved. A large sample area is measured, therefore decreasing the influence of inhomogeneities and providing a more representative sampling, for example polymer flakes and pellets.

For more granular and inhomogenous materials such as grains, an optical spinning sample cup is available to ensure the most representative sampling.

### Reliability and Reproducibility

The NIRA accessory eliminates the major problems associated with using fiber-optic probes for materials checking. Hand-held fiber optic probes are inherently unstable. The NIRA, however, offers a robust sampling platform. The automated self referencing feature also eliminates the need to collect separate background spectra.

Test data for replicate spectra of calcium ascorbate from a commercially available fiber optic probe system and the NIRA are shown in Figures 5 and 6. The results from the NIRA show much less variability than those of the probe system.

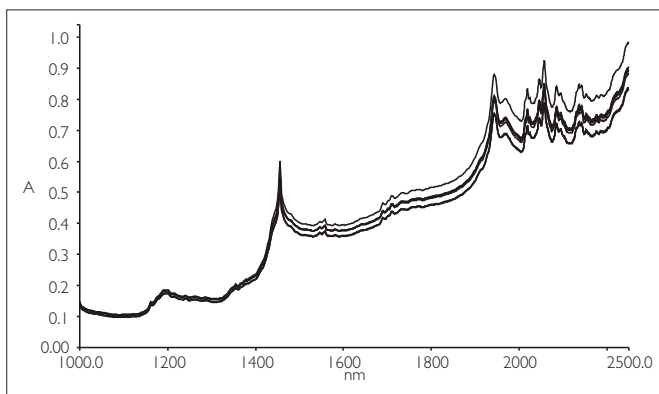


Figure 5. NIR spectra of calcium ascorbate in a glass bottle recorded using the NIRA.

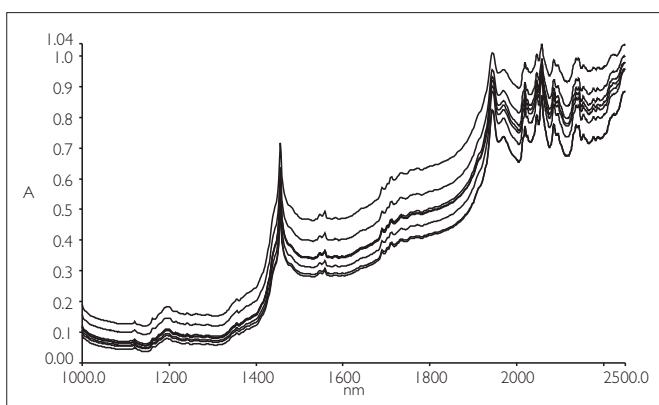


Figure 6. NIR spectra of calcium ascorbate recorded using a fiber optic solids probe.

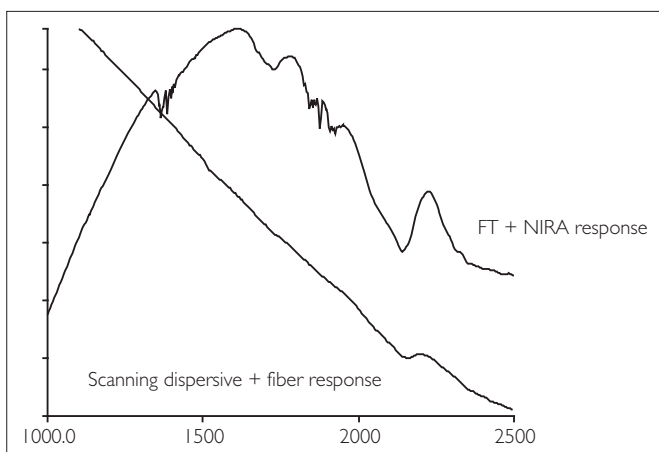


Figure 7. Typical response of the NIRA compared with a typical scanning dispersive instrument with a fiber probe.

## Spectral Response

Traditionally, NIR sampling has been confined to fiber optic and dispersive systems with spectra measuring between ca. 10000 – 2200 nm (10000 – 4545  $\text{cm}^{-1}$ ). These systems typically provide the highest response in the short wavelength region.

The response from the NIRA is shown in Figure 7 along with that of a typical dispersive system. Sample spectra are shown in Figures 8, 9 and 10 with the high quality long wavelength information gained when using the NIRA.

One advantage to this response allows for sampling to occur in original colored glass bottles which typically show spectra with little useful information in the shorter range. By collecting data in the longer wavelength region where the glass is transparent, sample identity can often be verified without removal from the original container. The NIRA is optimized for operation in the longer wavelength range in order to maximize the information content available.

## Resolution

The NIRA delivers new levels of information in NIR spectra due to the higher resolution available. In addition to improving spectral interpretation, this offers improved accuracy for qualitative analysis, and assists in transferring multivariate calibrations between instruments.

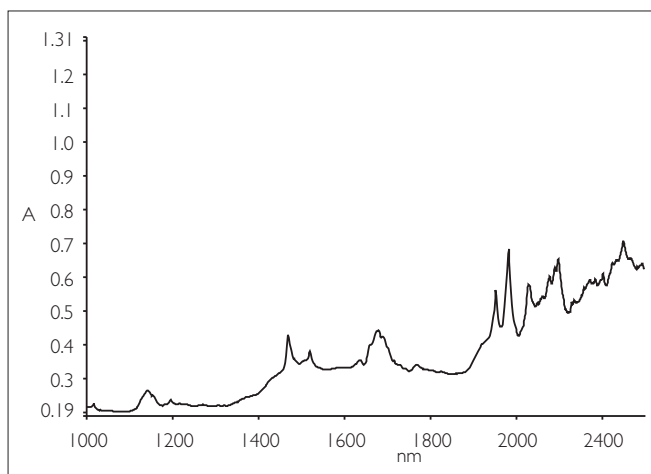


Figure 8. Tegretol® tablet.

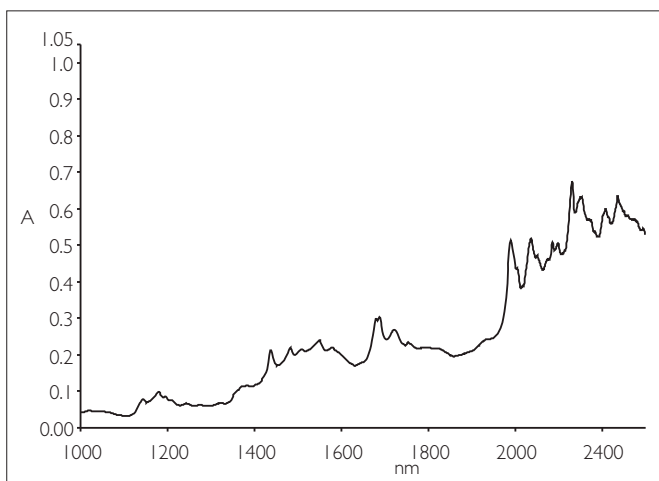


Figure 9. Procainamide tablet.

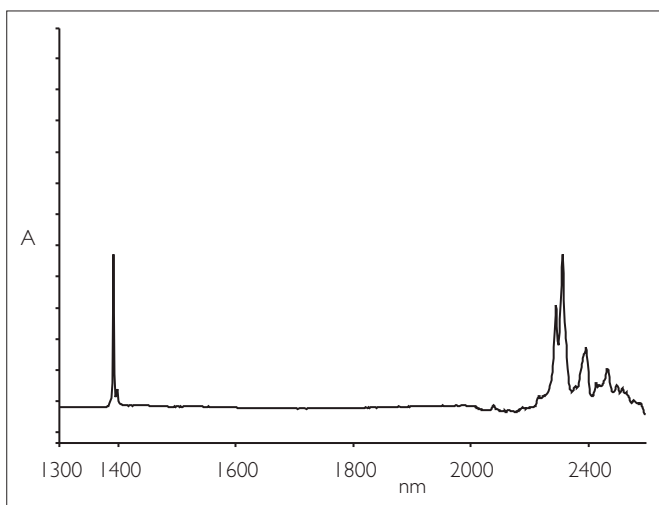


Figure 10. Talc.

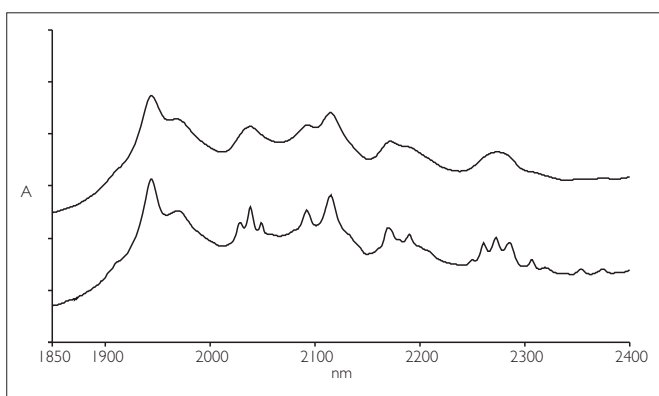


Figure 11. NIR spectra of calcium ascorbate at typical dispersive NIR instrument resolution 3 nm (upper) and FT resolution of 0.4 nm (lower).

## Conclusion

The NIRA offers simple but effective sampling solutions for materials testing without compromising spectral quality or time. The combination of optimized range and resolution reveals information which can potentially improve qualitative and quantitative applications. This extra level of spectral detail should provide new opportunities for analyses in terms of both easier sampling and improved spectral discrimination and quantitation.

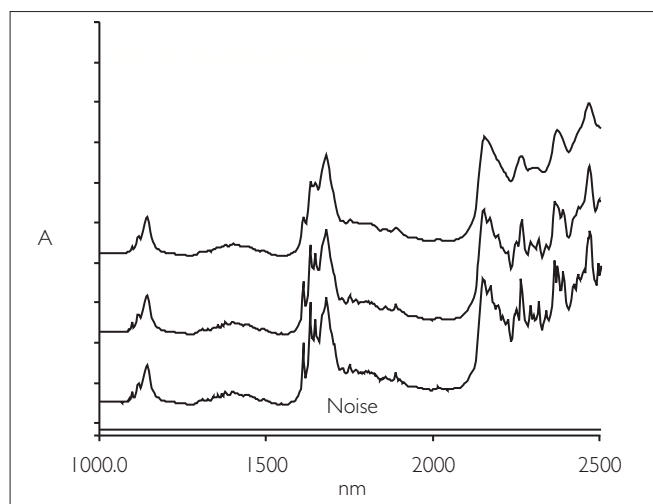


Figure 12. NIR spectra of clotrimazole at 4, 1.6, 0.8 nm resolution (upper to lower). The increased spectral information gained at higher resolution is real as the noise profile is shown on the same scale.

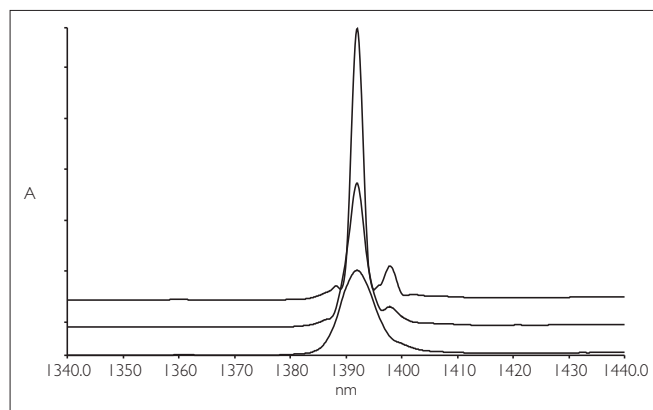


Figure 13. NIR spectra of talc at 0.4 nm, 1.6 nm and 3.2 nm resolution (upper to lower).

## FT-NIR Spectroscopy

## Author

J. Neal-Kababick

Flora Research Laboratories  
Grants Pass, OR USA

## Rapid Authentication of Botanicals for Dietary Supplement cGMP's Compliance by Automated FT-NIR Using Chemometric Modeling

### Introduction

Echinacea is one of the most popular botanical dietary supplements on the market. Several species and parts of the plant are used in the manufacturing of dietary supplements. In order to comply with Dietary Supplement current Good Manufacturing Practices (cGMP's), all dietary ingredients must be identified using valid scientific methods. For botanicals, this includes identifying the species and plant parts utilized for the dietary supplement. The cGMP's mandates that valid sampling plans must be utilized to produce representative laboratory samples. Botanicals are heterogeneous by nature, requiring multiple separate sample analyses to meet this mandate. Methods such as HPLC, microscopy and HPTLC are very effective but costly, time consuming and require hazardous chemicals. The PerkinElmer MIR/NIR spectrometer equipped with a NIR (near infrared) sampling accessory allows for rapid identification of Echinacea species and plant parts (i.e. root and aerial parts). The proper use of NIR coupled with a valid chemometric model using AssureID™ software meets the requirements of 21 CFR Part 11 and 21 CFR Part 111. Analysis time is less than one minute, is non-destructive and can be automated making NIR a realistic solution for multiple sample analyses of incoming material. It is important to note that this model is in development and additional samples will be added to expand the current library. Challenge samples were selected to demonstrate model abilities. Further work is in progress.

## Authentication of Dietary Supplement Ingredients

NIR is heavily utilized in numerous industries for material identification and quantitative analysis. In the dietary supplement industry, many issues have arisen with NIR due to improper instrumental use and data analysis. NIR authentication of botanical species requires the development of sample libraries using validated reference materials. A chemometric model must be developed and validated by challenge samples to assure success. While visual comparison of spectra is commonly utilized for MIR, this is inadequate for botanical authentication due to the inability to visualize subtle data differences in the NIR spectra.

A valid NIR method will accurately identify and pass authentic/in-specification material and reliably fail adulterated or out of specification material. Chemometric modeling with principle component analyses of data is required to do this. Once the model is developed, minimal operator skill is needed for routine analysis which can be performed by a properly trained technician. Failed samples can be investigated or rejected while passed samples can be released for further testing. This reduces costly upper level testing on non-compliant materials.

## Experimental

Materials used in this study are the following:

- Echinacea angustifolia root (various sources)
- Echinacea purpurea root (various sources)
- Echinacea purpurea tops (various sources)
- Echinacea pallida root (single source)

Piper methysticum root, Taraxacum off. root, E. purpurea seed and adulterated E. angustifolia root were also utilized.

The PerkinElmer MIR/NIR spectrometer is capable for both NIR and MIR operation, used with an NIR tablet autosampler or NIRA in combination with AssureID software.

Data acquisition was carried out using the following procedure:

- Collect background scan
- Place powdered sample in clear vial
- Place vial on NIRA or Tablet Autosampler
- Collect spectra and automatically process data

Powdered samples (40 mesh) were placed in scintillation vials and scanned on the tablet autosampler window in reflectance mode from 12,000  $\text{cm}^{-1}$  – 4000  $\text{cm}^{-1}$  in triplicate (25 scans each) at 8  $\text{cm}^{-1}$  resolution. Vial contents were shaken, tapped and scanned repeatedly (triplicate analyses). Data processing conditions were as follows: SIMCA algorithm, noise weighting, MSC normalization, first order derivative, 19 point width using the data range from 8,000  $\text{cm}^{-1}$  to 4000  $\text{cm}^{-1}$ .

## Results and Discussion

This model was able to properly identify materials. Primary materials were resolved by the NIR model. Additional samples of herb material and E. pallida would greatly enhance the model.

## Conclusion

NIR is a very powerful and rapid test method capable of valid identity testing of Echinacea species and plant parts. Data quality is dependent on the strength and quality of the model. Using the PerkinElmer MIR/NIR spectrometer and AssureID software allows for rapid development and deployment of valid identity test methods. Although still small, this model has already demonstrated the ability to distinguish different species and plant parts of Echinacea and foreign botanicals. Methods can be developed and tuned to account for specifications including particle size, moisture content, marker compound levels and other specifications as needed.

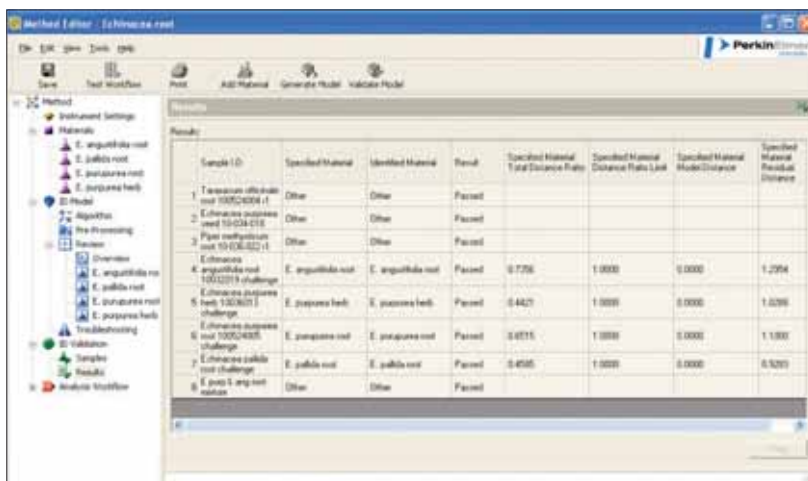


Figure 1. Results of ID validation for samples.

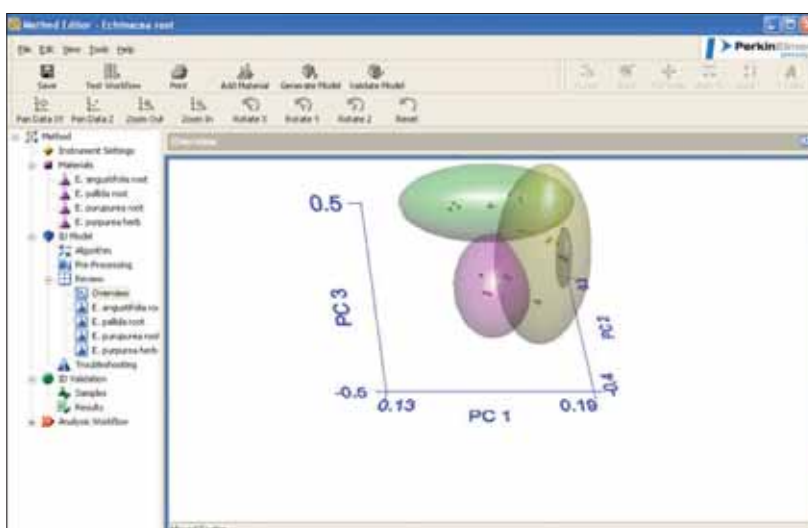


Figure 2. 3D Model of clusters. The software allows for rotation and zoom of display which confirms separation of clusters.

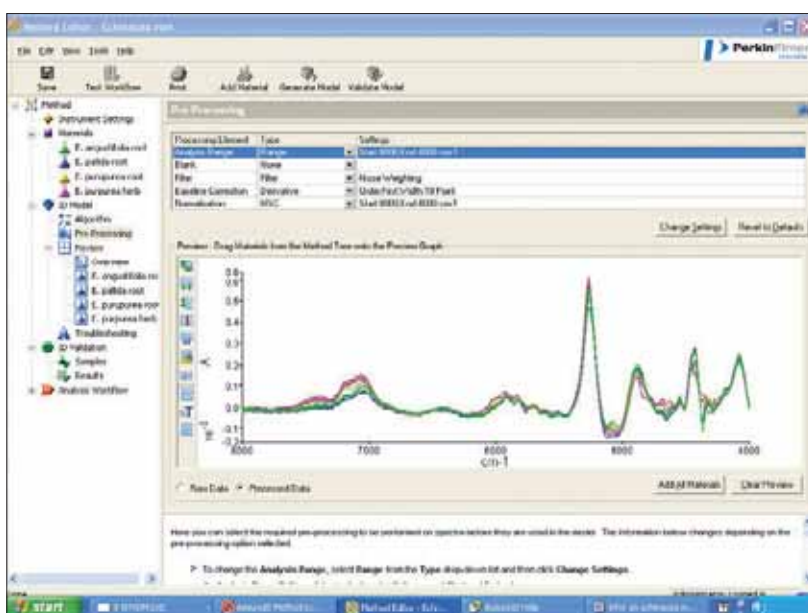


Figure 3. Preview of processed data (first order derivatives of Echinacea samples shown).

## References

1. Handbook of Near-Infrared Analysis, 3rd edition. Burns, D.A., Ciurczak, E.W., CRC press 2007.
2. Applied Chemometrics for Scientists. Brereton, R.G., Wiley 2007.
3. Federal Register – 21 CFR Part 111 (Code of Federal Regulations). <http://www.accessdata.fda.gov/scripts/cdrh/cfdocs/cfCFR/CFRSearch.cfm?CFRPart=111>
4. Chemometrics, A Practical Guide. Beebe, K.R., Pell, R.J., Seasholtz, M.B., Wiley 1998.

## Acknowledgement

A special thanks to Patrick Courtney, Ben Perston, and Jerry Sellors of PerkinElmer, Seer Green, for their invaluable assistance and support. Thanks to Cathy Sue Pekkala, Flora Research Laboratories, for sample preparation and data collection. Additional data showing Coomans Plot, residuals, raw data and sample reports available from the author.

**PerkinElmer, Inc.**  
940 Winter Street  
Waltham, MA 02451 USA  
P: (800) 762-4000 or  
(+1) 203-925-4602  
[www.perkinelmer.com](http://www.perkinelmer.com)



---

For a complete listing of our global offices, visit [www.perkinelmer.com/ContactUs](http://www.perkinelmer.com/ContactUs)

Copyright ©2010, PerkinElmer, Inc. All rights reserved. PerkinElmer® is a registered trademark of PerkinElmer, Inc. All other trademarks are the property of their respective owners.

009488\_01

## USEFUL LINKS

View previous issues of our Spotlight on Applications e-Zine

- Volume 1
- Volume 2
- Volume 3
- Volume 4
- Volume 5
- Volume 6
- Volume 7
- Archives

Access our application archives

### By Industry:

- Consumer Products
- Energy
- Environmental
- Food, Beverage & Nutraceuticals
- Forensics
- Lubricants
- Pharmaceutical Development & Manufacturing
- Polymers/Plastics
- Semiconductor & Electronics

### By Technology:

- Atomic Absorption (AA)
- Elemental Analysis
- Gas Chromatography (GC)
- GC Mass Spectrometry (GC/MS)
- Hyphenated Technology
- ICP Mass Spectrometry (ICP-MS)
- Inductively Coupled Plasma (ICP-OES & ICP-AES)
- Infrared Spectroscopy (FT-IR & IR)
- LIMS & Data Handling
- Liquid Chromatography (HPLC & UHPLC)
- Mass Spectrometry
- Raman Spectroscopy
- Thermal Analysis
- UV/Vis & UV/Vis/NIR

## ▶ NEW PinAAcle 900 AA Spectrometers

Unparalleled performance no matter the application

## ▶ Spectrum Two FT-IR

For applications in pharmaceuticals, polymers, nutraceutical and academia

PerkinElmer, Inc.  
940 Winter Street  
Waltham, MA 02451 USA  
P: (800) 762-4000 or  
(+1) 203-925-4602  
[www.perkinelmer.com](http://www.perkinelmer.com)



For a complete listing of our global offices, visit [www.perkinelmer.com/ContactUs](http://www.perkinelmer.com/ContactUs)

Copyright ©2011, PerkinElmer, Inc. All rights reserved. PerkinElmer® is a registered trademark of PerkinElmer, Inc. All other trademarks are the property of their respective owners.

009679\_02